



**TECHNISCHE
UNIVERSITÄT
DRESDEN**

Numerical Simulation of Reactive Transport Problems in Porous Media Using Global Implicit Approach

DISSERTATION

zur Erlangung des akademischen Grades

Doctor rerum naturalium
(Dr. rer. nat.)

vorgelegt

der Fakultät Umweltwissenschaften
der Technischen Universität Dresden

von

M.Sc. Reza Zolfaghari
Geb. am 07. April 1985 in Mashhad

Gutachter:
Prof. Dr.-Ing Olaf Kolditz
Dr. Haibing Shao
Dr. Amir Raouf

Eingereicht im November 2014

To My Beloved Parents and Wonderful Wife...

Declaration of Authorship

I hereby certify that the work presented here was conducted solely by myself and with the aid of the references listed.

Signed:

Date:

Acknowledgements

First of all I am grateful to my advisor Prof. Dr.-Ing Olaf Kolditz for providing me with the means to work on this fascinating subject. I am grateful to Dr. Haibing Shao and Dr. Serge Kräutle for their invaluable guidances at the early stage of my PhD. This work was not possible without their helps in the first place. I am thankful to Dr. Norihiro Watanabe for answering many questions on the structure and further development of OGS⁶ software. Next I thank Dr. Wenqing Wang, and Dr. Dmitri Naumov for the many valuable discussions I had with them on various aspects of this work. Furthermore, I am thankful to my wife Zakia, my family and friends (esp. Mostafa and Mesbah) for their continuous mental supports. Finally, I am very grateful to the secretaries Sindy Bleiholder, Nora Eigenwill, and the rest of colleagues in the department of environmental informatics (ENVINF) for making my stay at Helmholtz Centre a great working and learning experience.

Leipzig November 2014

Reza Zolfaghari

Abstract

This thesis focuses on solutions of reactive transport problems in porous media. The principle mechanisms of flow and reactive mass transport in porous media are investigated. Global implicit approach (GIA), where transport and reaction are fully coupled, and sequential non-iterative approach (SNIA) are implemented into the software OpenGeoSys (OGS⁶) to couple chemical reaction and mass transport. The reduction scheme proposed by Krättele is used in GIA to reduce the number of coupled nonlinear differential equations. The reduction scheme takes linear combinations within mobile species and immobile species and effectively separates the reaction-independent linear differential equations from coupled nonlinear ones (i.e. reducing the number of primary variables in the nonlinear system). A chemical solver is implemented using semi-smooth Newton iteration which employs complementarity condition to solve for equilibrium mineral reactions. The results of three benchmarks are used for code verification. Based on the solutions of these benchmarks, it is shown that GIA with the reduction scheme is faster (ca. 6.7 times) than SNIA in simulating homogeneous equilibrium reactions and (ca. 24 times) in simulating kinetic reaction. In simulating heterogeneous equilibrium mineral reactions, SNIA outperforms GIA with the reduction scheme by 4.7 times.

Zusammenfassung

Diese Arbeit konzentriert sich auf die numerische Berechnung reaktiver Transportprobleme in porösen Medien. Es werden prinzipielle Mechanismen von Fluidströmung und reaktive Stofftransport in porösen Medien untersucht. Um chemische Reaktionen und Stofftransport zu koppeln, wurden die Ansätze Global Implicit Approach (GIA) sowie Sequential Non-Iterative Approach (SNIA) in die Software OpenGeoSys (OGS⁶) implementiert. Das von Krättele vorgeschlagene Reduzierungsschema wird in GIA verwendet, um die Anzahl der gekoppelten nichtlinearen Differentialgleichungen zu reduzieren. Das Reduzierungsschema verwendet Linearkombinationen von mobilen und immobile Spezies und trennt die reaktionsunabhängigen linearen Differentialgleichungen von den gekoppelten nichtlinearen Gleichungen (dh Verringerung der Anzahl der Primärvariablen des nicht-linearen Gleichungssystems). Um die Gleichgewichtsreaktionen der Mineralien zu berechnen, wurde ein chemischer Gleichungslser auf Basis von "semi-smooth Newton-Iterations" implementiert. Ergebnisse von drei Benchmarks wurden zur Code-Verifikation verwendet. Diese Ergebnisse zeigen, dass die Simulation homogener Equilibriumreaktionen mit GIA 6,7 mal schneller und bei kinetischen Reaktionen 24 mal schneller als SNIA sind. Bei Simulationen heterogener Equilibriumreaktionen ist SNIA 4,7 mal schneller als der GIA Ansatz.

Contents

Declaration of Authorship	iii
Acknowledgements	iv
Abstract	v
List of Figures	viii
Symbols	ix
1 Introduction	1
1.1 State of the Art	1
1.2 Thesis Objectives	3
1.3 Thesis Outline	4
2 Mathematical Models	5
2.1 Introduction	5
2.2 Mass Balance Equations	5
2.2.1 Groundwater Flow	6
2.2.2 Mass Transport	7
2.2.3 Chemical Reaction	8
2.2.3.1 Equilibrium Reaction	8
2.2.3.2 Kinetic Reaction	10
2.3 Reactive Mass Transport	10
2.4 Initial and Boundary Conditions	11
3 Numerical Solutions	12
3.1 Introduction	12
3.2 Coupling Schemes	12
3.2.1 Operator Splitting	13
3.2.2 Global Implicit	13
3.2.2.1 Standard Reduction Schemes	14
3.2.2.2 Kräutle’s Reduction Scheme	14
3.2.2.3 Local Chemical Solver	21
3.3 Space and Time Discretization	23

3.3.1	Finite Element Method	23
3.3.2	Time Discretization	25
3.3.3	Jacobian Matrix	26
3.4	Code Implementation	29
4	Benchmarks	30
4.1	Introduction	30
4.2	Cation Exchange	30
4.3	Dissolution and Precipitation	32
4.4	Mixing Controlled Biodegradation	33
5	Conclusions and Outlooks	38
5.1	Conclusions	38
5.2	Outlooks	39

List of Figures

3.1	Algorithm applied for calculating the local residual.	23
3.2	Algorithm used for modified Newton's method with line search.	24
3.3	One time step of the reduction scheme.	28
4.1	Breakthrough curves of concentrations in the cation exchange benchmark . . .	31
4.2	Aqueous concentration profiles for dissolution and precipitation benchmark . .	33
4.3	Calcite and dolomite profiles for dissolution and precipitation benchmark . . .	34
4.4	CPU time measured versus number of nodes in simulating mineral dissolution and precipitation benchmark	34
4.5	Simulation domain for mixing controlled biodegradation benchmark	36
4.6	Transverse profiles of compounds in mixing controlled biodegradation benchmark	36
4.7	Transverse profiles of biomass in mixing controlled biodegradation benchmark	37
4.8	CPU time in simulating mixing controlled biodegradation benchmark	37

Symbols

Symbol	Name	Unit
\mathbf{A}_1	matrix from relation (3.9), size: $(J_{mob} + J_{sorp,li} + J_{min} + J_{1,kin}^*) \times J_{sorp}$	-
$\mathbf{A}_{1,kin}$	submatrix of \mathbf{A}_1 , size: $J_{1,kin}^* \times J_{kin}$	-
$\mathbf{A}_{1,min}$	submatrix of \mathbf{A}_1 , size: $J_{min} \times J_{kin}$	-
$\mathbf{A}_{1,mob}$	submatrix of \mathbf{A}_1 , size: $J_{sorp,li} \times J_{kin}$	-
\mathbf{A}_2	matrix from relation (3.9), size: $(J_{sorp} + J_{min} + J_{2,kin}^*) \times J$	-
$\mathbf{A}_{2,kin}$	submatrix of \mathbf{A}_2 , size: $J_{2,kin}^* \times J_{kin}$	-
$\mathbf{A}_{2,sorp}$	submatrix of \mathbf{A}_2 , size: $J_{sorp} \times J_{kin}$	-
$\mathbf{A}_{2,sorp,ld}$	submatrix of $\mathbf{A}_{2,sorp}$, size: $(J_{sorp} - J_{sorp,li}) \times J_{kin}$	-
$\mathbf{A}_{2,sorp,li}$	submatrix of $\mathbf{A}_{2,sorp}$, size: $J_{sorp,li} \times J_{kin}$	-
\mathbf{A}_{ld}	matrix from relation (3.7), size: $J_{min} \times (J_{sorp} - J_{sorp,li})$	-
α_l	longitudinal dispersivity	(m)
α_t	transversal dispersivity	(m)
\mathbf{c}	concentration vector of mobile species, length: I	(kg/m ³)
$\bar{\mathbf{c}}$	concentration vector of immobile species, length: \bar{I}	(kg/m ³)
$\bar{\mathbf{c}}_{min}$	concentration vector of minerals, length: \bar{I}_{min}	(kg/m ³)
$\bar{\mathbf{c}}_{nmin}$	concentration vector of nonminerals, length: \bar{I}_{nmin}	(kg/m ³)
\mathbf{D}_i	diffusion/dispersion tensor of the i^{th} species	(m ² /s)
η	transformed variables (mobile reaction invariants), size: $I - J_{mob} - J_{sorp,li} - J_{min} - J_{1,kin}^*$	-
$\bar{\eta}$	transformed variables (immobile reaction invariants), size: $\bar{I} - J_{sorp} - J_{min} - J_{2,kin}^*$	-
I	number of mobile species	-
\bar{I}	number of immobile species	-
\bar{I}_{min}	number of minerals	-
\bar{I}_{nmin}	number of nonminerals	-
\mathbf{I}_n	identity matrix of size n	-
J	number of chemical reactions	-

J_{eq}	number of equilibrium reactions	-
J_{kin}	number of kinetic reactions	-
$J_{1,kin}^*$	number of columns of $\mathbf{S}_{1,kin}^*$	-
$J_{2,kin}^*$	number of columns of $\mathbf{S}_{2,kin}^*$	-
J_{min}	number of equilibrium mineral reactions	-
J_{mob}	number of equilibrium homogeneous mobile reactions	-
J_{sorp}	number of equilibrium sorption reactions	-
$J_{sorp,li}$	number of columns of $\mathbf{S}_{1,sorp,li}$	-
K_j	equilibrium constant of the j -th equilibrium reaction	-
L	linear transport operator	-
l	logarithms of the mobile concentrations, vector length: I	-
l_{nmin}	logarithms of the nonmineral concentrations, vector length: I_{nmin}	-
Λ	diagonal matrix with reciprocal values of mobile concentrations	-
$\bar{\Lambda}_{nmin}$	diagonal matrix with reciprocal values of nonminerals concentrations	-
$\tilde{\Lambda}$	diagonal matrix containing (Λ and $\bar{\Lambda}_{nmin}$)	-
\mathbf{n}	outer normal	-
Ω	computational domain	-
ϕ_j	j -th equilibrium condition	-
ϕ	vector of all equilibrium conditions, length: J_{eq}	-
ϕ_{min}	equilibrium conditions of mineral reactions, number: J_{min}	-
ϕ_{mob}	equilibrium conditions of homogeneous mobile reactions, number: J_{mob}	-
ϕ_{sorp}	equilibrium conditions of sorption reactions, number: J_{sorp}	-
ψ_j	equilibrium condition of the j -th mineral reaction in presence of mineral	-
\mathbf{q}	Darcy flow	(m/s)
\mathbf{r}	reaction rate vector, length: J	-
\mathbf{r}_{eq}	reaction rates of equilibrium reactions, number: J_{eq}	-
$\mathbf{r}_{kin}(\mathbf{c}, \bar{\mathbf{c}})$	reaction rates of kinetic reactions, number: J_{kin}	-
\mathbf{S}	stoichiometric matrix with entries of mobile species, size: $(I + \bar{I}) \times J$	-
\mathbf{S}_1	submatrix of \mathbf{S} , size: $I \times J$	-
$\mathbf{S}_{1,eq}$	submatrix of \mathbf{S}_{eq} , size: $I \times J_{eq}$	-
$\mathbf{S}_{1,kin}$	submatrix of \mathbf{S}_{kin} , size: $I \times J_{kin}$	-
$\mathbf{S}_{1,kin}^*$	submatrix of \mathbf{S}_1^* with entries of kinetic reactions, size: $I \times J_{1,kin}^*$	-
$\mathbf{S}_{1,min}$	submatrix of $\mathbf{S}_{1,eq}$ with entries of mineral reactions, size: $I \times J_{min}$	-
$\mathbf{S}_{1,min,A}$	submatrix of $\mathbf{S}_{1,min}$ with active reactions (minerals are not present)	-
$\mathbf{S}_{1,min,I}$	submatrix of $\mathbf{S}_{1,min}$ with inactive reactions (minerals are present)	-
$\mathbf{S}_{1,mob}$	submatrix of $\mathbf{S}_{1,eq}$ with equilibrium only mobile reactions, size: $I \times J_{mob}$	-
\mathbf{S}_1^\perp	matrix with max. system orthogonal to \mathbf{S}_1^* , size: $I \times (I - J_{mob} - J_{sorp,li} - J_{min} - J_{1,kin}^*)$	-
\mathbf{S}_1^*	matrix with max. system of linear independent columns of \mathbf{S}_1 , size:	-

	$I \times (J_{mob} + J_{sorp,li} + J_{min} + J_{1,kin}^*)$	
$\mathbf{S}_{1,sorp}$	submatrix of $\mathbf{S}_{1,eq}$ with entries of sorption reactions, size: $I \times J_{sorp}$	-
$\mathbf{S}_{1,sorp,li}$	submatrix of $\mathbf{S}_{1,sorp}$ with entries of sorption reactions, size: $I \times J_{sorp,li}$	-
\mathbf{S}_2	submatrix of \mathbf{S} with entries of immobile species, size: $\bar{I} \times J$	-
$\mathbf{S}_{2,eq}$	submatrix of \mathbf{S}_{eq} with entries of immobile species, size: $\bar{I} \times J_{eq}$	-
$\mathbf{S}_{2,kin}$	submatrix of \mathbf{S}_{kin} with entries of immobile species, size: $\bar{I} \times J_{kin}$	-
$\mathbf{S}_{2,kin}^*$	submatrix of \mathbf{S}_{kin}^* with entries of nonminerals and kinetic reactions, size: $\bar{I}_{nmin} \times J_{2,kin}^*$	-
\mathbf{S}_2^\perp	matrix with max. system orthogonal to \mathbf{S}_2^* , size: $\bar{I} \times (\bar{I} - J_{sorp} - J_{min} - J_{2,kin}^*)$	-
\mathbf{S}_2^*	matrix with max. system of linear independent columns of \mathbf{S}_2 , size: $\bar{I} \times (J_{sorp} + J_{min} + J_{2,kin}^*)$	-
$\mathbf{S}_{2,sorp}$	submatrix of $\mathbf{S}_{2,eq}$ with entries of nonminerals and sorption reactions, size: $\bar{I}_{nmin} \times J_{sorp}$	-
\mathbf{S}_{eq}	submatrix of \mathbf{S} with entries of equilibrium reactions, size: $(I + \bar{I}) \times J_{eq}$	-
\mathbf{S}_{kin}	submatrix of \mathbf{S} with entries of kinetic reactions, size: $(I + \bar{I}) \times J_{kin}$	-
θ^w	water content	-
Δt	time step size	S
ξ	transformed variables, number of var.: $J_{mob} + J_{sorp,li} + J_{min} + J_{1,kin}^*$	-
$\bar{\xi}$	transformed variables, number of var.: $J_{sorp} + J_{min} + J_{2,kin}^*$	-
$\bar{\xi}_{kin}$	transformed variables, number of var.: $J_{2,kin}^*$	-
$\bar{\xi}_{min}$	transformed variables, number of var.: J_{min}	-
$\bar{\xi}_{sorp}$	transformed variables, number of var.: J_{sorp}	-
$\bar{\xi}_{sorp,ld}$	transformed variables, number of var.: $J_{sorp,ld}$	-
$\bar{\xi}_{sorp,li}$	transformed variables, number of var.: $J_{sorp,li}$	-
ξ_{glob}	global variables, number of var.: $J_{mob} + J_{sorp,li} + J_{min} + J_{1,kin}^*$	-
ξ_{kin}	transformed variables, number of var.: $J_{1,kin}^*$	-
ξ_{loc}	local variables, number of var.: $J_{mob} + J_{sorp} + J_{min} + J_{2,kin}^*$	-
ξ_{min}	transformed variables, number of var.: J_{min}	-
ξ_{mob}	transformed variables, number of var.: J_{mob}	-
ξ_{sorp}	transformed variables, number of var.: $J_{sorp,li}$	-
$\tilde{\xi}$	transformed variables, number of var.: $J_{sorp,li} + J_{min}$	-
$\tilde{\xi}_{min}$	transformed variables, number of var.: J_{min}	-
$\tilde{\xi}_{sorp}$	transformed variables, number of var.: $J_{sorp,li}$	-

Chapter 1

Introduction

Numerical modeling plays an essential role in many science and engineering fields since experiments are usually too slow, too expensive, dangerous or even impossible to perform under difficult controlled experimental conditions. Computer simulations are used to quantitatively and qualitatively understand and predict natural phenomena such as transport processes in aquifer and reservoirs by taking into account heat and mass transfer as well as the associated chemical reactions.

Of particular interest to earth and environment scientists and engineers is the ability to evaluate and predict spatial and temporal distribution of conserved properties such as mass (chemical compounds), energy and heat in porous structures such as soil and concrete. Application examples include: in safety assessment of nuclear disposal sites, CO₂ storage sites, and remediation of contaminated groundwater.

These conserved properties can be mathematically expressed through differential equations. These equations are then discretized to be solved through computer simulations. The simulation results are later used for numerical analysis.

1.1 State of the Art

There are two general ways to handle mass balance equations of reactive transport processes. One is known as the global implicit approach (GIA) where mass transport and chemical reactions are solved together (fully coupled approach) in one system of equations [SL94]. The other method is the so-called operator splitting (OS) approach where mass transport and chemical reactions (decoupled approach) are solved separately one after the other [SCA01]. In operator splitting sequential non-iterative approach (SNIA), solution of linear transport step is followed

by solution of nonlinear chemistry on each node at each time step. On the other hand, in operator splitting sequential iterative approach (SIA), iteration between solutions of transport and chemistry is performed until an error tolerance is met [CMB04].

The advantages of OS methods are its easy implementation and less demands of computational resources in terms of memory and CPU time. However, decoupling of mass transport and chemical reaction processes introduces splitting error [CMB04, SL06, SL07]. This error has two components, an error associated with the boundary and an error within the domain [SL07]. The OS error in kinetic reaction systems tends to smooth concentration fronts if transport is solved before reaction or steepen concentration fronts if the reaction is solved first [SL06, SL08]. This OS error, which is independent of grid discretization error, is controlled by reaction rate and time step size [KM95, MK95, VM92, XSA⁺99]. The OS error can be removed if alternating OS schemes, where the sequence of solving transport and reaction is changing, is used in kinetically controlled reaction systems [SL06, SL07, SL08]. When handling equilibrium reaction systems, the OS error is the largest in simulating heterogeneous equilibrium reactions and can be decreased by taking smaller time step sizes or using SIA [HK89].

SIA is an attractive way to remove the splitting error if sufficiently small time step sizes are taken [HK89, YT89]. Xu et al. [XSA⁺99] compared SIA with SNIA in solving a number of different chemical equilibrium reaction systems. Their results showed the computation time of SNIA is half of SIA depending on desired accuracy, nature of the reactions, temporal and spatial discretization.

Over 25 years ago, Yeh and Tripathi [YT89] compared GIA with SIA based on their CPU time, memory consumption and implementation effort. Their theoretical analysis favored SIA over GIA due to excessive computation time and memory requirement of GIA in realistic multi-dimensional applications and ease of implementation and modification of SIA in handling mixed equilibrium and kinetic reaction systems. However, using Picard method, SIA needs more iterations per time step to converge. SIA, contrary to GIA, is stiffer in chemically complex systems (highly nonlinear or very retarded) which requires very small time step sizes to converge [RK88, SM96]. Saaltink et al. [SCA00, SCA01] compared SIA and GIA for a number of problems with a varying degree of complexity. Based on their results they concluded that GIA is faster and more accurate than SIA for chemically complex system while with simple chemistry and large number of grids, SIA outperforms GIA.

GIA is mass conservative and is less restricted by time step size. However, the major drawback of GIA is the high cost of computational resources when solving a large system of equations in each iteration. A common practice to mitigate this problem is to isolate nonlinear chemical reaction terms to as few equations as possible through linear combination of mass balance equations [FR92]. This reformulation usually reduces the number of coupled nonlinear PDEs by decoupling of linear component equations and elimination of unknown equilibrium reaction rates.

Component equations are best derived as the column vectors of the orthogonal complement of the stoichiometric subspace of the concentration space [AM63, FR92].

Such a reduction algorithm for complex mixed equilibrium and kinetic reaction systems in open systems (*i.e.* groundwater) was published in the work of Friedly [Fri91] and Friedly and Rubin [FR92] for the first time. Their reduction scheme, however, suffers from appearance of nonlinearity and coupling terms under transport operator, which destroys the sparsity of Jacobian matrix leading to an increase in cost of computational resources, or restrictive assumption on the equilibrium reaction types, such that their reduction scheme fails in a reaction systems containing reactions within the aqueous phase and between the aqueous and solid phases [KK05].

These problems were solved in the new reduction scheme of Kräutle and Knabner [KK05, KK07], and Kräutle [Krä08] who proposed a separate reformulation and introduction of new variables within the block of mass balance equations for mobile and immobile components and species. To further reduce the size of the coupled nonlinear partial differential equations (PDEs), they used a local chemical solver to solve for some local variables consisting of algebraic equations (AEs) and ordinary differential equations (ODEs) and then substituted them in the time derivative and kinetic rate terms of the remaining global coupled nonlinear PDEs [Hof10, HKK10, KK07]. The total number of coupled nonlinear PDEs in the new reduction scheme equals the sum of linearly independent heterogeneous equilibrium and kinetic reactions and it is independent of the number of homogeneous equilibrium reactions [Hof10, KK07]. The MoMaS benchmark competition revealed that the GIA with the new reduction scheme requires less CPU time compared to other standard GIA, SIA and SNIA based codes in simulating strongly nonlinear and heterogeneous reactive transport problems [CHK⁺10, HKK10, HKK12].

For efficient numerical simulation of chemical system containing equilibrium mineral reactions, mineral equilibrium conditions are considered as complementarity conditions (CCs) where CCs are transformed into equivalent algebraic equation and then the whole nonlinear system of equations is solved by semi-smooth Newton method [BKKK11, Hof10, HKK10, KK07, Krä08].

1.2 Thesis Objectives

The objective of this work is to implement the GIA with reduction scheme presented in [Hof10] into the OGS⁶ software and compare it to the conventional SNIA in simulating different reactive transport scenarios.

1.3 Thesis Outline

- Chapter 1 highlights the importance of computer simulations and state of the art in simulating reactive transport problems.
- Chapter 2 contains mass balance equations for mass and chemistry.
- Chapter 3 briefly introduces mass transport and chemistry coupling and reduction schemes, space and time discretization, the assembly of the Jacobian matrix, and the implementation strategy.
- Chapter 5 presents 3 benchmarks.

Chapter 2

Mathematical Models

2.1 Introduction

Continuum mechanics is based on conservation laws of extensive state quantities such as mass, momentum and energy. These conservation laws are, however, transferred into measured intensive quantities (e.g. concentration, temperature, density, pressure, viscosity, etc). Equation of state relates extensive and intensive state quantities. The basic mathematical equations used to solve for fluid flow under isothermal, constant density, single phase and fully saturated condition at subsurface environment is briefly presented in this chapter. Isothermal and isobaric conditions are considered for chemical reactions.

2.2 Mass Balance Equations

The general conservation law from Eulerian perspective states that the rate of change of an extensive quantity in a fixed control volume equals net fluxes across the control volume plus the source and sink term. Mathematically it can be expressed as [Kol02]:

$$\frac{\partial}{\partial t} \int_{\Omega} \rho d\Omega + \oint_{\partial\Omega} \mathbf{n} \cdot \mathbf{f} d\Omega = \int_{\Omega} s d\Omega \quad (2.1)$$

where ρ is volumetric density, \mathbf{n} normal unit vector, \mathbf{f} flux density, and volume-specific source/sink term s . Applying the Gaussian divergence theorem the surface integral is transformed to volume integral.

$$\int_{\Omega} \frac{\partial}{\partial t} \rho d\Omega + \int_{\Omega} \nabla \cdot \mathbf{f} d\Omega = \int_{\Omega} s d\Omega \quad (2.2)$$

Choosing an infinitesimally small control volume (i.e. point) the general mass balance formulation can be written in its differential form:

$$\frac{\partial}{\partial t}\rho + \nabla \cdot \mathbf{f} = s \quad (2.3)$$

2.2.1 Groundwater Flow

Subsurface environment (i.e. earth) is consist of solid and void space and water only flows within the pore space (n_e). Considering fully saturated condition ($n_e = \theta^w$) where all the pores are filled with water (i.e. no gas), Darcy's law holds [Bea72]

$$\mathbf{q} = -\mathbf{K}\nabla h \quad (2.4)$$

with \mathbf{K} hydraulic conductivity and ∇h hydraulic gradient and the balance equation after equation 2.3 for water mass ($= \theta^w \rho^w$) can be written as:

$$\frac{\partial}{\partial t}(\theta^w \rho^w) + \nabla \cdot (\rho^w \mathbf{q}) = \rho^w q_0 \quad (2.5)$$

with specific discharge \mathbf{q} and injection or extraction rate q_0 . Extending the above equation and dividing by water density ρ^w one gets:

$$\frac{\partial}{\partial t}\theta^w + \frac{\theta^w}{\rho^w} \frac{\partial}{\partial t}\rho^w + \frac{1}{\rho^w} \nabla \rho^w \cdot \mathbf{q} + \nabla \cdot \mathbf{q} = q_0 \quad (2.6)$$

Considering slightly compressible fluid and neglecting spatial density gradient ($\nabla \rho^w$), the chain rule can be applied to the temporal derivatives to include hydraulic head (primary variable):

$$\left(\frac{\partial}{\partial h}\theta^w + \frac{\theta^w}{\rho^w} \frac{\partial}{\partial h}\rho^w\right) \frac{\partial}{\partial t}h + \nabla \cdot \mathbf{q} = q_0 \quad (2.7)$$

Substituting equation 2.4 into 2.7 yields the three-dimensional groundwater flow equation:

$$S_0 \frac{\partial}{\partial t}h - \nabla \cdot (\mathbf{K}\nabla h) = q_0 \quad (2.8)$$

where S_0 ($S_0 = \frac{\partial}{\partial h}\theta^w + \frac{\theta^w}{\rho^w} \frac{\partial}{\partial h}\rho^w$) is the specific storage coefficient.

2.2.2 Mass Transport

The extensive quantity considered is mass of solute ($= n_e c$) which is concentration of solute times effective porosity or volumetric water content (θ^w) in a fully saturated condition. Concentration of mobile species (c) and immobile species (\bar{c}) are expressed in mole per volume water (Molarity) to avoid any extra conversion step. Following the mass conservation equation 2.3 the mass balance for mobile species (I) is expressed by partial differential equation (PDE) [Yeh00]:

$$\frac{\partial}{\partial t}(\theta^w c_i) + \nabla \cdot (\mathbf{q}c_i - \theta^w \mathbf{D}_i \nabla c_i) = s_i, \quad i = 1, \dots, I \quad (2.9)$$

where \mathbf{q} is specific discharge or Darcy velocity, s_i is source and sink including chemical reactions ($s_i = c_i^{in} q_{in} - c_i q_{out} + \sum_{j=1}^J \theta^w S_{ij} r_j$, with inflow concentration c_i^{in} and chemical reactions J), and \mathbf{D}_i is the Scheidegger diffusion/dispersion tensor expressed as [Bea72]:

$$\mathbf{D}_i = \underbrace{(\theta^w D_e^d)}_{\text{dif. coef.}} + \underbrace{\alpha_l |\mathbf{q}| \mathbf{I} + (\alpha_l - \alpha_t) \frac{\mathbf{q} \otimes \mathbf{q}}{|\mathbf{q}|}}_{\text{dispersion coefficient}} \quad (2.10)$$

where D_e^d is the effective molecular diffusion coefficient (considering tortuosity), α_l and α_t are longitudinal and transverse dispersivities, respectively. The mass flux density consists of advective ($\mathbf{q}c_i$) and diffusive/dispersive terms ($-\theta^w \mathbf{D}_i \nabla c_i$). Advection is the transport of solute by Darcy flow. Diffusion is the random Brownian motion of solute particles in fluids (i.e. the natural tendency toward equilibrium and homogeneity). Dispersion is the spreading and mixing of solute caused by velocity fluctuations during advection. The effect of dispersion on spreading and mixing solute is much larger than the effect of diffusion (dispersion coefficient \gg diffusion coefficient).

Mass balance for the immobile species (\bar{I}) is expressed with ordinary differential equations (ODE) as:

$$\frac{\partial}{\partial t}(\theta^w \bar{c}_i) = \sum_{j=1}^J \theta^w S_{ij} r_j, \quad i = I + 1, \dots, I + \bar{I} \quad (2.11)$$

where S_{ij} is the stoichiometric coefficient (a constant numbers indicating quantitative contributions of each species in chemical reactions) and r_j is the j th chemical reaction. Mobile and immobile species are coupled through chemical reactions (right hand site source and sink terms s_i of equation 2.11).

2.2.3 Chemical Reaction

The nonlinearities in the solute transport equations 2.9 and 2.11 come from the chemical reactions (source/sink term) which cause the transformation of reactive species in the system. Chemical reactions can be categorized into kinetic reactions and equilibrium reactions based on their rates. If the characteristic time of reaction is slower than time scale of transport, the reaction is said to be kinetically controlled and if characteristic time of reaction is much faster than characteristic time of transport, the reaction is at local equilibrium. Dimensionless Damköhler numbers (e.g. comparison of reaction rate to advection rate results in $\frac{\lambda L_a}{v}$, with first order rate coefficient λ , length L_a , and velocity v) are used to relate characteristic time scale of advection, dispersion and reaction with each others [Las98]. Based on the number of phases a reaction involves, chemical reaction can also be divided to homogeneous (aqueous phase) and heterogeneous reactions (aqueous-solid phases). A general classification of reactions can be found in [Rub83].

2.2.3.1 Equilibrium Reaction

Assuming local equilibrium reactions, the thermodynamic concentrations (activities) of educts and products are in a fixed ratio at every point of the simulation domain. Law of mass action (LMA) relates the products activities of a reaction to activities of educts as:

$$\ln(K_j) = \sum_{i=1}^{I+\bar{I}} S_{ij} \ln(a_i) \quad (2.12)$$

where K is equilibrium constant and a_i is activity or thermodynamic concentration. The influence of temperature and pressure on equilibrium constant can be found in standard text books (e.g. [SM12]). Since equilibrium reaction rates (\mathbf{r}_{eq}) are unknowns, we substitute the following equations with the solute mass balance equations (2.9) and (2.11) that contains equilibrium reaction rates \mathbf{r}_{eq} :

$$\phi_j(\mathbf{c}, \bar{\mathbf{c}}) = -\ln(K_j) + \sum_{i=1}^{I+\bar{I}} S_{ij} \ln(a_i) = 0 \quad (2.13)$$

Activity Correction

activity a_i is the fraction of total concentration c_i which participates in a reaction. Activity coefficient γ_i relates activity to concentration as:

$$a_i = \gamma_i c_i \quad (2.14)$$

Assuming ideal solution the activity of solid minerals and pure water phase are considered unity. Activity coefficient is a function of ionic strength I_s which corresponds to mineralization degree of a solution and can be calculated as:

$$I_s = 0.5 \sum_i^I c_i z_i^2 \quad (2.15)$$

where c_i in a non-ideal solution is molar concentrations and z_i is the charge of ionic species i . Debye-Hückel (for $I_s < 0.1$) and Davies equations (for $I_s < 0.5$) are used to calculate activity coefficients. Debye-Hückel equation reads [Bet07]

$$\log \gamma_i = -Az_i^2 \frac{\sqrt{I_s}}{1 + Bb_i \sqrt{I_s}} \quad (2.16)$$

where A, B are temperature-dependent constants, and b_i is ion-size parameter. Davies equation reads

$$\log \gamma_i = -Az_i^2 \left(\frac{\sqrt{I_s}}{1 + \sqrt{I_s}} - 0.3I_s \right) \quad (2.17)$$

Equilibrium Mineral Reactions

The LMA also applies if minerals are involved in equilibrium reactions. Stoichiometric coefficients of minerals are set to positive one (minerals are put on the right hand side of reactions and their equilibrium constant signs are flipped) and their activities are considered unity (ideal solid solution). Furthermore, it is assumed that only one mineral is involved in any reaction. LMA reads

$$\psi_j(\mathbf{c}) = -\ln(K_j) + \sum_{i=1}^I S_{ij} \ln(a_i) = 0 \quad (2.18)$$

In this case the equilibrium condition, consisting of equation and inequality, reads

$$\underbrace{(\psi_j(\mathbf{c}) = 0, \bar{c}_{min,j} \geq 0)}_{saturated} \vee \underbrace{(\psi_j(\mathbf{c}) > 0, \bar{c}_{min,j} = 0)}_{undersaturated} \quad (2.19)$$

where $c_{min,j}$ is the concentration of mineral in j -th equilibrium reaction. Assume a solution to be undersaturated with respect to a mineral ($\psi_j(\mathbf{c}) > 0$), The LMA pushes the solution to dissolve the mineral in order to reach saturated or equilibrium condition ($\psi_j(\mathbf{c}) = 0$) or total dissolution of the mineral ($c_{min,j} = 0$).

In order to solve the system of equations and inequalities 2.19 Krättele [Krä08] proposed to use complementarity condition. Accordingly 2.19 can be rewritten as:

$$\forall_j = 1, \dots, J_{min} : \psi_j(\mathbf{c}) \geq 0 \wedge \bar{c}_{min,j} \geq 0 \wedge \psi_j(\mathbf{c}) \bar{c}_{min,j} = 0 \quad (2.20)$$

where J_{min} is the number of mineral reactions. Minimum function was used to transform complementarity condition to algebraic equation (AE) [Krä11]:

$$\phi_j(\mathbf{c}, \bar{\mathbf{c}}) = \min(\psi_j(\mathbf{c}), c_{min,j}) = 0 \quad (2.21)$$

which states equilibrium condition is achieved, if $\phi_j(\mathbf{c}, \bar{\mathbf{c}}) = 0$. Equation 2.21 is replaced for the solute mass balance equations containing equilibrium mineral reaction rates.

2.2.3.2 Kinetic Reaction

In case of kinetic bio-reaction, double Monod expression is considered. Considering a simple reaction $\frac{1}{Y_s}C_s + \frac{1}{Y_a}C_a \xrightarrow{X} C_p$ where biomass X in the presence of substrate (C_s) and electron acceptor (C_a) (i.e. oxygen, nitrate, etc) produces some product (C_p) and constant biomass decay, the mass balance equations for Monod type expression reads [CV07]

$$k_{gr} = \mu_{max} \left(\frac{C_s}{K_s + C_s} \right) \left(\frac{C_a}{K_a + C_a} \right) \quad (2.22a)$$

$$\frac{\partial}{\partial t} C_s = -\frac{k_{gr}}{Y_s} X \quad (2.22b)$$

$$\frac{\partial}{\partial t} C_a = -\frac{k_{gr}}{Y_a} X \quad (2.22c)$$

$$\frac{\partial}{\partial t} X = k_{gr} X - k_{dec} X \quad (2.22d)$$

where $\mu_{max}[T^{-1}]$ is the maximum growth rate, K_s and K_a are Monod coefficients, k_{gr} and k_{dec} are the specific growth and decay rates of biomass.

2.3 Reactive Mass Transport

Considering chemical reactions as the sole source and sink terms of solute mass balance equations 2.9 and 2.11 and a mixed equilibrium and kinetic reaction system, the source and sink terms read

$$s_i = \sum_{j=1}^{J_{eq}} \theta^w S_{eq,ij} r_j + \sum_{j=1}^{J_{kin}} \theta^w S_{kin,ij} r_j(\mathbf{c}, \bar{\mathbf{c}}) \quad (2.23)$$

Where equilibrium reactions are considered first followed by kinetic reactions. Furthermore considering mobile species I (index 1 in (2.24)) before immobile species \bar{I} (index 2 in (2.24)), the stoichiometric coefficients in matrix notation can be written as:

$$\mathbf{S} = \begin{pmatrix} \mathbf{S}_{eq} & \mathbf{S}_{kin} \end{pmatrix} = \begin{pmatrix} \mathbf{S}_1 \\ \mathbf{S}_2 \end{pmatrix} = \begin{pmatrix} \mathbf{S}_{1,eq} & \mathbf{S}_{1,kin} \\ \mathbf{S}_{2,eq} & \mathbf{S}_{2,kin} \end{pmatrix} \quad (2.24)$$

where \mathbf{S} is the stoichiometric coefficient matrix with its rows corresponding to species ($I + \bar{I}$) and its columns to chemical reactions ($J = J_{eq} + J_{kin}$). The source and sink terms read

$$\mathbf{s} = \theta^w \begin{pmatrix} \mathbf{S}_{1,eq} & \mathbf{S}_{1,kin} \\ \mathbf{S}_{2,eq} & \mathbf{S}_{2,kin} \end{pmatrix} \begin{pmatrix} \mathbf{r}_{eq} \\ \mathbf{r}_{kin} \end{pmatrix} \quad (2.25)$$

with \mathbf{r} ($J \times 1$) the vector of reaction rates. Representing the linear transport operator with $L_i c_i := \nabla \cdot (\mathbf{q} c_i - \mathbf{D}_i \nabla c_i)$, the reactive solute mass balance equations 2.9 and 2.11 can be written as

$$\frac{\partial}{\partial t}(\theta^w \mathbf{c}) + L\mathbf{c} = \theta^w \mathbf{S}_{1,eq} \mathbf{r}_{eq} + \theta^w \mathbf{S}_{1,kin} \mathbf{r}_{kin}(\mathbf{c}, \bar{\mathbf{c}}) \quad (2.26)$$

$$\frac{\partial}{\partial t}(\theta^w \bar{\mathbf{c}}) = \theta^w \mathbf{S}_{2,eq} \mathbf{r}_{eq} + \theta^w \mathbf{S}_{2,kin} \mathbf{r}_{kin}(\mathbf{c}, \bar{\mathbf{c}}) \quad (2.27)$$

$$\phi(\mathbf{c}, \bar{\mathbf{c}}) = 0 \quad (2.28)$$

where equation 2.26 is a set of nonlinear partial differential equations (PDE), equation 2.27 is a set of nonlinear ordinary differential equations, and equation 2.28 is a set of nonlinear algebraic equations (AE).

2.4 Initial and Boundary Conditions

In order to solve differential equations, boundary (PDE) and initial (PDE in transient case and ODE) conditions need to be specified. Dirichlet and Neumann boundary conditions are considered for solute transport and flow as

$$c(x) = c_{fix}(x) \text{ at } \Gamma_D \quad (2.29)$$

$$h(x) = h_{fix}(x) \text{ at } \Gamma_D \quad (2.30)$$

$$\mathbf{D} \nabla c \cdot \mathbf{n} = 0 \text{ at } \Gamma_N \quad (2.31)$$

$$-\mathbf{K} \nabla h \cdot \mathbf{n} = q_{fix} \text{ at } \Gamma_N, \quad (2.32)$$

where \mathbf{n} is the normal unit vector pointing outwards.

Chapter 3

Numerical Solutions

3.1 Introduction

Numerical solutions are usually used in practice due to the limiting assumptions of analytical solutions such as homogeneous and geometrically simple media. Mass transport and reaction coupling techniques and numerical schemes for space and time discretizations are briefly presented in this chapter.

3.2 Coupling Schemes

Coupling of fluid flow and reactive transport is performed sequentially, using Picard linearization, as

$$\mathbf{K}_p \mathbf{p} = \mathbf{f}_p$$

$$\mathbf{K}_u \mathbf{u} = \mathbf{f}_u$$

where reactive transport is solved following the solution of groundwater flow.

The conservative mass transport and reaction are solved using fully coupled method (i.e. GIA) or in a decoupled manner (i.e. SNIA). The sequential coupling is performed non-iteratively where the solution of a conservative mass transport is followed by the solution of chemistry at each time step. The global coupling or so-called global implicit approach (GIA) solves mass transport and chemistry in one step which requires Newton type of linearization techniques and construction of Jacobian matrix.

3.2.1 Operator Splitting

In operator splitting method the linear mass transport and nonlinear chemical reactions (2.9) are solved separately one after the other as

$$\frac{c_i^{n*} - c_i^n}{\Delta t} = L_i(c_i^n) \quad (3.1)$$

$$\frac{c_i^{n+1} - c_i^{n*}}{\Delta t} = s_i(c_i^{n*}) \quad (3.2)$$

The changes due to scalar transport operator and nonlinear local chemical reactions are applied to the stored mass sequentially and non-iteratively hence the method is called sequential non-iterative approach (SNIA). Due to the decoupling of transport and chemistry, SNIA requires less computational resources in terms of memory and time compared to standard GIA. In reality transport of compounds and chemical reactions are occurring at the same time and a decoupled approach such as SNIA introduces splitting error. Furthermore, since an explicit time integration method is used, SNIA is constrained with Courant-Friedrichs-Lewy condition or in short Courant (Cr) number ($= \frac{v\Delta t}{\Delta x} \leq 1$) [SM96]. Cr number condition states that the concentration front from one cell must move to the neighboring cell in downstream direction at each time step to avoid numerical dispersion.

In order to avoid splitting error and Cr constraint, sequential iterative approach (SIA) can be applied where an iteration between transport (3.1) and chemistry (3.2) is performed until a convergence criterion is met. The drawback of SIA is the large number of iterations or stability and efficiency issues [SCA00, SCA01, CMB04].

3.2.2 Global Implicit

To avoid the potential disadvantages of SNIA and SIA, GIA is used which is considered to be more robust. In GIA, mass transport and chemistry are solved together using implicit time integration scheme as

$$\frac{c_i^{n+1} - c_i^n}{\Delta t} = L_i(c_i^{n+1}) + s_i(c_i^{n+1}) \quad (3.3)$$

GIA is mass conservative and using implicit backward Euler time integration scheme, it is less constrained by time step size or Cr number. The drawbacks of GIA stems from the nonlinearity nature of chemistry which requires linearization techniques (e.g. Newton scheme) in order to solve (3.3). Newton scheme is known to be quadratically converging compared to Picard scheme if the initial guess is close to the final solution. It, however, consists of solving a large linear system of equations ($\mathbf{Ax} = \mathbf{b}$) (with a degree of freedom (DOF) equals number of nodes \times number

of species) at each iteration which is computationally expensive in terms of time and memory resources.

In reality hundreds of species can be present in a mixed kinetic and equilibrium reactive system with unknown equilibrium reaction rates. Hence, in order to reduce the computational burden, a common method is to eliminate equilibrium reaction rates and separate the linear equations (non-reactive ones) and nonlinear equations (reactive ones) through component matrix, which will be explained in the next section. The procedure is called reduction scheme due to the reduction of the number of nonlinear PDEs. A common assumption of all reduction schemes (due to the combination of equations) is that the diffusion coefficient is the same for all species. This assumption is made because in Scheidegger diffusion-dispersion tensor (2.10), diffusion coefficient is orders of magnitude smaller than dispersion coefficient.

3.2.2.1 Standard Reduction Schemes

The core idea behind reduction schemes are to take linear combinations of mass balance equations such that conservative component equations occur and nonlinear reaction terms are eliminated from some of the equations [Fri91, FR92, SAC98, FYB03, MCAS04, KK05]. In matrix notation, it can be expressed as to find a matrix \mathbf{S}^\perp whose columns are orthogonal to all columns of stoichiometric matrix \mathbf{S} , i.e.,

$$\mathbf{S}^{\perp T} \mathbf{S} = 0 \quad (3.4)$$

Matrix \mathbf{S}^\perp is called component matrix (mobile and immobile species in \mathbf{S} are not sorted as in (2.25)). The inverse of matrices \mathbf{S}^\perp and \mathbf{S} are multiplied with the mass balance equations (2.9) and (2.11) in order to decouple some linear PDEs from the rest of the nonlinear PDEs. Due to the mixing of mobile and immobile species either decoupling is not possible [MCAS04] or coupling and nonlinearity is happening under the transport operator [Fri91, FR92, KK05].

3.2.2.2 Kräutle's Reduction Scheme

In order to solve the restrictions and inefficiencies mentioned in previous subsection, Kräutle and Knabner [KK05] proposed to separate mobile and immobile species in the stoichiometric matrix and calculate the orthogonal complement matrix \mathbf{S}^\perp within the mobile and immobile block of stoichiometric matrix. Their strategy was to reduce the combination of mobile and immobile species as much as possible during the decoupling phase. A complete avoidance of taking combination of mobile and immobile species is, however, not possible due to implicit nature of equilibrium reaction rate. Furthermore, no combination of mobile and immobile species is appearing under transport operator in their reduction scheme which makes their scheme computationally more efficient and robust [KK05, KK07, Krä08].

The following assumptions are made for the reduction scheme

- diffusion coefficient is the same for all species.
- linear independence is assumed for homogeneous equilibrium and heterogeneous equilibrium mineral reactions.
- equilibrium mineral and sorbed species do not participate in a kinetic reaction. So the stoichiometric coefficients related to minerals and sorbed species are zero in stoichiometric matrix of kinetic reactions.
- Only one mineral is participating in a mineral reaction and mineral is considered as products i.e. positive signs are given in stoichiometric matrix (leads to identity matrix in (3.6)) and hence the sign of equilibrium reaction constant has to be adjusted accordingly.

Concentrations of mobile species come first in the concentration vector followed by the concentrations of immobile species pertaining to sorption, kinetic and mineral reactions as

$$\begin{pmatrix} \mathbf{c} \\ \bar{\mathbf{c}} \end{pmatrix}, \quad \bar{\mathbf{c}} = \begin{pmatrix} \bar{\mathbf{c}}_{sorp} \\ \bar{\mathbf{c}}_{kin} \\ \bar{\mathbf{c}}_{min} \end{pmatrix} \quad (3.5)$$

Equilibrium reactions are sorted in the following way. First homogeneous equilibrium reactions are listed followed by heterogeneous equilibrium sorption and mineral reactions

$$\mathbf{S}_{1,eq} = \begin{pmatrix} \mathbf{S}_{1,mob} & \mathbf{S}_{1,sorp} & \mathbf{S}_{1,min} \end{pmatrix}, \quad \mathbf{S}_{2,eq} = \begin{pmatrix} 0 & \mathbf{S}_{2,sorp} & 0 \\ 0 & 0 & \mathbf{I}_{J_{min}} \end{pmatrix} \quad (3.6)$$

where $\mathbf{I}_{J_{min}}$ is an identity matrix of the size J_{min} (due to the last assumption).

It is assumed that $\mathbf{S}_{1,sorp} = \begin{pmatrix} \mathbf{S}_{1,sorp,li} & \mathbf{S}_{1,min} \mathbf{A}_{ld} \end{pmatrix}$ with a coefficient matrix \mathbf{A}_{ld} such that the columns of $\begin{pmatrix} \mathbf{S}_{1,mob} & \mathbf{S}_{1,sorp,li} & \mathbf{S}_{1,min} \end{pmatrix}$ are linear independent.

Then the stoichiometric coefficient matrix (2.24) is

$$\begin{aligned} \mathbf{S}_1 &= \begin{pmatrix} \mathbf{S}_{1,eq} & \mathbf{S}_{1,kin} \end{pmatrix} = \begin{pmatrix} \mathbf{S}_{1,mob} & \mathbf{S}_{1,sorp,li} & \mathbf{S}_{1,min} \mathbf{A}_{ld} & \mathbf{S}_{1,min} & \mathbf{S}_{1,kin} \end{pmatrix} \\ \mathbf{S}_2 &= \begin{pmatrix} \mathbf{S}_{2,eq} & \mathbf{S}_{2,kin} \end{pmatrix} = \begin{pmatrix} 0 & \mathbf{S}_{2,sorp} & 0 & 0 \\ 0 & 0 & 0 & \mathbf{S}_{2,kin} \\ 0 & 0 & \mathbf{I}_{J_{min}} & 0 \end{pmatrix} \end{aligned} \quad (3.7)$$

Now the matrices \mathbf{S}_1^* and \mathbf{S}_2^* are defined such that each contains a maximal system of linear independent columns of \mathbf{S}_1 and \mathbf{S}_2 , respectively. Due to linear independence assumptions of equilibrium reactions, the matrices \mathbf{S}_1^* and \mathbf{S}_2^* can be written as

$$\begin{aligned} \mathbf{S}_1^* &= \begin{pmatrix} \mathbf{S}_{1,mob} & \mathbf{S}_{1,sorp,li} & \mathbf{S}_{1,min} & \mathbf{S}_{1,kin}^* \end{pmatrix} \\ \mathbf{S}_2^* &= \begin{pmatrix} \mathbf{S}_{2,sorp} & 0 & 0 \\ 0 & 0 & \mathbf{S}_{2,kin}^* \\ 0 & \mathbf{I}_{J_{min}} & 0 \end{pmatrix} \end{aligned} \quad (3.8)$$

There are always matrices \mathbf{A}_1 and \mathbf{A}_2 such that

$$\mathbf{S}_i = \mathbf{S}_i^* \mathbf{A}_i \quad i = 1, 2 \quad (3.9)$$

where \mathbf{A}_i can be calculated as

$$\mathbf{A}_i = \left(\mathbf{S}_i^{*T} \mathbf{S}_i^* \right)^{-1} \mathbf{S}_i^{*T} \mathbf{S}_i \quad i = 1, 2 \quad (3.10)$$

and has block structure

$$\begin{aligned} \mathbf{A}_1 &= \begin{pmatrix} \mathbf{I}_{J_{mob}} & 0 & 0 & 0 & \mathbf{A}_{1,mob} \\ 0 & \mathbf{I}_{J_{sorp,li}} & 0 & 0 & \mathbf{A}_{1,sorp} \\ 0 & 0 & \mathbf{A}_{ld} & \mathbf{I}_{J_{min}} & \mathbf{A}_{1,min} \\ 0 & 0 & 0 & 0 & \mathbf{A}_{1,kin} \end{pmatrix} \\ \mathbf{A}_2 &= \begin{pmatrix} 0 & \mathbf{I}_{J_{sorp}} & 0 & \mathbf{A}_{2,sorp} \\ 0 & 0 & \mathbf{I}_{J_{min}} & 0 \\ 0 & 0 & 0 & \mathbf{A}_{2,kin} \end{pmatrix} \end{aligned} \quad (3.11)$$

After rearranging the coefficient matrices, the matrices \mathbf{S}_1^\perp and \mathbf{S}_2^\perp are calculated. The matrices \mathbf{S}_1^\perp and \mathbf{S}_2^\perp consist of a maximal system of linear independent vectors that are orthogonal to all columns of \mathbf{S}_1^* and \mathbf{S}_2^* , respectively, such that

$$\mathbf{S}_i^{\perp T} \mathbf{S}_i^* = 0 \quad i = 1, 2 \quad (3.12)$$

Substituting 3.9 into the mass balance equations

$$\begin{aligned} \frac{\partial}{\partial t}(\theta^w \mathbf{c}) + L\mathbf{c} &= \theta^w \mathbf{S}_1^* \mathbf{A}_1 \mathbf{r} \\ \frac{\partial}{\partial t}(\theta^w \bar{\mathbf{c}}) &= \theta^w \mathbf{S}_2^* \mathbf{A}_2 \mathbf{r} \end{aligned} \quad (3.13)$$

and multiplication of the inverse of orthogonal complement matrices \mathbf{S}_i^\perp (component matrices) with the system of mass balance equations eliminates the nonlinear reaction terms from right

hand side of the differential equations

$$\begin{aligned} \left(\mathbf{S}_1^{\perp T} \mathbf{S}_1^{\perp}\right)^{-1} \mathbf{S}_1^{\perp T} \left(\frac{\partial}{\partial t}(\theta^w \mathbf{c}) + L\mathbf{c}\right) &= \theta^w \underbrace{\left(\mathbf{S}_1^{\perp T} \mathbf{S}_1^{\perp}\right)^{-1} \mathbf{S}_1^{\perp T} \mathbf{S}_1^* \mathbf{A}_1 \mathbf{r}}_{=0} \\ \left(\mathbf{S}_2^{\perp T} \mathbf{S}_2^{\perp}\right)^{-1} \mathbf{S}_2^{\perp T} \frac{\partial}{\partial t}(\theta^w \bar{\mathbf{c}}) &= \theta^w \underbrace{\left(\mathbf{S}_2^{\perp T} \mathbf{S}_2^{\perp}\right)^{-1} \mathbf{S}_2^{\perp T} \mathbf{S}_2^* \mathbf{A}_2 \mathbf{r}}_{=0} \end{aligned} \quad (3.14)$$

and multiplying the inverses of \mathbf{S}_i^* with the mass balance equations yields

$$\begin{aligned} \left(\mathbf{S}_1^{*T} \mathbf{S}_1^*\right)^{-1} \mathbf{S}_1^{*T} \left(\frac{\partial}{\partial t}(\theta^w \mathbf{c}) + L\mathbf{c}\right) &= \theta^w \underbrace{\left(\mathbf{S}_1^{*T} \mathbf{S}_1^*\right)^{-1} \mathbf{S}_1^{*T} \mathbf{S}_1^* \mathbf{A}_1 \mathbf{r}}_{=\mathbf{I}} \\ \left(\mathbf{S}_2^{*T} \mathbf{S}_2^*\right)^{-1} \mathbf{S}_2^{*T} \frac{\partial}{\partial t}(\theta^w \bar{\mathbf{c}}) &= \theta^w \underbrace{\left(\mathbf{S}_2^{*T} \mathbf{S}_2^*\right)^{-1} \mathbf{S}_2^{*T} \mathbf{S}_2^* \mathbf{A}_2 \mathbf{r}}_{=\mathbf{I}} \end{aligned} \quad (3.15)$$

where \mathbf{I} is identity matrix. These manipulations correspond to the taking linear combinations of mass balance equations 3.13 within the blocks of equations related to mobile and immobile species.

The \mathbf{S}_i^* and \mathbf{S}_i^{\perp} matrices and the differential operators in system 3.14 and 3.15 commute because mobile and immobile species are not mixed and are constant in space and time. Hence new variables are defined as

$$\begin{aligned} \boldsymbol{\eta} &:= \left(\mathbf{S}_1^{\perp T} \mathbf{S}_1^{\perp}\right)^{-1} \mathbf{S}_1^{\perp T} \mathbf{c}, & \boldsymbol{\xi} &:= \left(\mathbf{S}_1^{*T} \mathbf{S}_1^*\right)^{-1} \mathbf{S}_1^{*T} \mathbf{c} \\ \bar{\boldsymbol{\eta}} &:= \left(\mathbf{S}_2^{\perp T} \mathbf{S}_2^{\perp}\right)^{-1} \mathbf{S}_2^{\perp T} \bar{\mathbf{c}}, & \bar{\boldsymbol{\xi}} &:= \left(\mathbf{S}_2^{*T} \mathbf{S}_2^*\right)^{-1} \mathbf{S}_2^{*T} \bar{\mathbf{c}} \end{aligned} \quad (3.16)$$

where $\boldsymbol{\eta}$ and $\bar{\boldsymbol{\eta}}$ are mobile and immobile reaction invariants (i.e. components), respectively, and $\boldsymbol{\xi}$ and $\bar{\boldsymbol{\xi}}$ are reaction extends withing mobile and immobile phases, respectively.

with retransformation we get

$$\mathbf{c} = \mathbf{S}_1^* \boldsymbol{\xi} + \mathbf{S}_1^{\perp} \boldsymbol{\eta}, \quad \bar{\mathbf{c}} = \mathbf{S}_2^* \bar{\boldsymbol{\xi}} + \mathbf{S}_2^{\perp} \bar{\boldsymbol{\eta}}, \quad (3.17)$$

The number of columns of \mathbf{S}_1^{\perp} and \mathbf{S}_2^{\perp} matrices equals the number of entries of $\boldsymbol{\eta}$ and $\bar{\boldsymbol{\eta}}$ vectors, respectively. \mathbf{S}_1^{\perp} has $I - J_{mob} - J_{sorp,li} - J_{min} - J_{1,kin}^*$ and \mathbf{S}_2^{\perp} has $\bar{I} - J_{sorp} - J_{min} - J_{2,kin}^*$ columns. The number of columns of \mathbf{S}_1^* and \mathbf{S}_2^* matrices equals the number of entries of $\boldsymbol{\xi}$ and $\bar{\boldsymbol{\xi}}$ vectors, respectively. \mathbf{S}_1^* has $J_{mob} + J_{sorp,li} + J_{min} + J_{1,kin}^*$ and \mathbf{S}_2^* has $J_{sorp} + J_{min} + J_{2,kin}^*$ columns. The vectors $\begin{pmatrix} \boldsymbol{\xi} \\ \boldsymbol{\eta} \end{pmatrix}$ and $\begin{pmatrix} \bar{\boldsymbol{\xi}} \\ \bar{\boldsymbol{\eta}} \end{pmatrix}$ are representations of the vectors \mathbf{c} and $\bar{\mathbf{c}}$ regarding to another basis of the \mathbb{R}^I and $\mathbb{R}^{\bar{I}}$, respectively.

So the system of equations 3.14 and 3.15 can be written as

$$\frac{\partial}{\partial t}(\theta^w \boldsymbol{\eta}) + L\boldsymbol{\eta} = 0 \quad (3.18)$$

$$\frac{\partial}{\partial t}(\theta^w \bar{\boldsymbol{\eta}}) = 0 \quad (3.19)$$

$$\frac{\partial}{\partial t}(\theta^w \boldsymbol{\xi}) + L\boldsymbol{\xi} = \theta^w \mathbf{A}_1 \mathbf{r} \quad (3.20)$$

$$\frac{\partial}{\partial t}(\theta^w \bar{\boldsymbol{\xi}}) = \theta^w \mathbf{A}_2 \mathbf{r} \quad (3.21)$$

where the linear component equations (reaction invariants) 3.18 and 3.19 are decoupled from the nonlinear differential equations (reaction extends) 3.20 and 3.21. Eq. 3.18 is a set of linear PDEs, 3.19 linear ODEs, 3.20 coupled nonlinear PDEs, and 3.21 nonlinear ODEs.

Linear component equations was decoupled so far. A further reduction of unknown equilibrium reaction rates \mathbf{r}_{eq} from \mathbf{r} in equations 3.20 and 3.21 (see also 2.26 and 2.27) is possible by partitioning $\boldsymbol{\xi}$ and $\bar{\boldsymbol{\xi}}$ analogously to \mathbf{S}_i^* , and \mathbf{r}_{eq} analogously to $\mathbf{S}_{1,eq}$ as

$$\boldsymbol{\xi} = \begin{pmatrix} \boldsymbol{\xi}_{mob} \\ \boldsymbol{\xi}_{sorp} \\ \boldsymbol{\xi}_{min} \\ \boldsymbol{\xi}_{kin} \end{pmatrix}, \quad \bar{\boldsymbol{\xi}} = \begin{pmatrix} \bar{\boldsymbol{\xi}}_{sorp} \\ \bar{\boldsymbol{\xi}}_{min} \\ \bar{\boldsymbol{\xi}}_{kin} \end{pmatrix}, \quad \mathbf{r}_{eq} = \begin{pmatrix} \mathbf{r}_{mob} \\ \mathbf{r}_{sorp} \\ \mathbf{r}_{min} \end{pmatrix} \quad (3.22)$$

Furthermore, analogously to $\mathbf{S}_{1,sorp}$, vectors $\bar{\boldsymbol{\xi}}_{sorp} = \begin{pmatrix} \bar{\boldsymbol{\xi}}_{sorp,li} \\ \bar{\boldsymbol{\xi}}_{sorp,ld} \end{pmatrix}$ and $\mathbf{r}_{sorp} = \begin{pmatrix} \mathbf{r}_{sorp,li} \\ \mathbf{r}_{sorp,ld} \end{pmatrix}$ are partitioned. Accordingly $\mathbf{A}_{2,sorp}$ is splitted in two submatrix of $\mathbf{A}_{2,sorp,li}$ containing the first $J_{sorp,li}$ rows and $\mathbf{A}_{2,sorp,ld}$ containing the last $(J_{sorp} - J_{sorp,li})$ rows of $\mathbf{A}_{2,sorp}$.

Using the mentioned partitioned vectors and the block structure of \mathbf{A}_i (3.11) one get

$$\begin{aligned} \frac{\partial}{\partial t}(\theta^w \boldsymbol{\eta}) + L\boldsymbol{\eta} &= 0 \\ \frac{\partial}{\partial t}(\theta^w \bar{\boldsymbol{\eta}}) &= 0 \\ \frac{\partial}{\partial t} \left(\theta^w \begin{pmatrix} \boldsymbol{\xi}_{mob} \\ \boldsymbol{\xi}_{sorp} \\ \boldsymbol{\xi}_{min} \\ \boldsymbol{\xi}_{kin} \end{pmatrix} \right) + L \begin{pmatrix} \boldsymbol{\xi}_{mob} \\ \boldsymbol{\xi}_{sorp} \\ \boldsymbol{\xi}_{min} \\ \boldsymbol{\xi}_{kin} \end{pmatrix} &= \theta^w \begin{pmatrix} \mathbf{I}_{J_{mob}} & 0 & 0 & 0 & \mathbf{A}_{1,mob} \\ 0 & \mathbf{I}_{J_{sorp,li}} & 0 & 0 & \mathbf{A}_{1,sorp} \\ 0 & 0 & \mathbf{A}_{ld} & \mathbf{I}_{J_{min}} & \mathbf{A}_{1,min} \\ 0 & 0 & 0 & 0 & \mathbf{A}_{1,kin} \end{pmatrix} \begin{pmatrix} \mathbf{r}_{mob} \\ \mathbf{r}_{sorp,li} \\ \mathbf{r}_{sorp,ld} \\ \mathbf{r}_{min} \\ \mathbf{r}_{kin}(\mathbf{c}, \bar{\mathbf{c}}) \end{pmatrix} \\ \frac{\partial}{\partial t} \left(\theta^w \begin{pmatrix} \bar{\boldsymbol{\xi}}_{sorp} \\ \bar{\boldsymbol{\xi}}_{min} \\ \bar{\boldsymbol{\xi}}_{kin} \end{pmatrix} \right) &= \theta^w \begin{pmatrix} 0 & \mathbf{I}_{J_{sorp}} & 0 & \mathbf{A}_{2,sorp} \\ 0 & 0 & \mathbf{I}_{J_{min}} & 0 \\ 0 & 0 & 0 & \mathbf{A}_{2,kin} \end{pmatrix} \begin{pmatrix} \mathbf{r}_{mob} \\ \mathbf{r}_{sorp} \\ \mathbf{r}_{min} \\ \mathbf{r}_{kin}(\mathbf{c}, \bar{\mathbf{c}}) \end{pmatrix} \end{aligned}$$

Expanding the above system of equations leads to

$$\frac{\partial}{\partial t}(\theta^w \boldsymbol{\eta}) + L\boldsymbol{\eta} = 0 \quad (3.23)$$

$$\frac{\partial}{\partial t}(\theta^w \bar{\boldsymbol{\eta}}) = 0 \quad (3.24)$$

$$\frac{\partial}{\partial t}(\theta^w \boldsymbol{\xi}_{mob}) + L\boldsymbol{\xi}_{mob} = \theta^w (\mathbf{r}_{mob} + \mathbf{A}_{1,mob} \mathbf{r}_{kin}(\mathbf{c}, \bar{\mathbf{c}})) \quad (3.25)$$

$$\frac{\partial}{\partial t}(\theta^w \boldsymbol{\xi}_{sorp}) + L\boldsymbol{\xi}_{sorp} = \theta^w (\mathbf{r}_{sorp,li} + \mathbf{A}_{1,sorp} \mathbf{r}_{kin}(\mathbf{c}, \bar{\mathbf{c}})) \quad (3.26)$$

$$\frac{\partial}{\partial t}(\theta^w \boldsymbol{\xi}_{min}) + L\boldsymbol{\xi}_{min} = \theta^w (\mathbf{r}_{min} + \mathbf{A}_{ld} \mathbf{r}_{sorp,ld} + \mathbf{A}_{1,min} \mathbf{r}_{kin}(\mathbf{c}, \bar{\mathbf{c}})) \quad (3.27)$$

$$\frac{\partial}{\partial t}(\theta^w \boldsymbol{\xi}_{kin}) + L\boldsymbol{\xi}_{kin} = \theta^w \mathbf{A}_{1,kin} \mathbf{r}_{kin}(\mathbf{c}, \bar{\mathbf{c}}) \quad (3.28)$$

$$\frac{\partial}{\partial t}(\theta^w \bar{\boldsymbol{\xi}}_{sorp,li}) = \theta^w (\mathbf{r}_{sorp,li} + \mathbf{A}_{2,sorp,li} \mathbf{r}_{kin}(\mathbf{c}, \bar{\mathbf{c}})) \quad (3.29)$$

$$\frac{\partial}{\partial t}(\theta^w \bar{\boldsymbol{\xi}}_{sorp,ld}) = \theta^w (\mathbf{r}_{sorp,ld} + \mathbf{A}_{2,sorp,ld} \mathbf{r}_{kin}(\mathbf{c}, \bar{\mathbf{c}})) \quad (3.30)$$

$$\frac{\partial}{\partial t}(\theta^w \bar{\boldsymbol{\xi}}_{min}) = \theta^w \mathbf{r}_{min} \quad (3.31)$$

$$\frac{\partial}{\partial t}(\theta^w \bar{\boldsymbol{\xi}}_{kin}) = \theta^w \mathbf{A}_{2,kin} \mathbf{r}_{kin} \quad (3.32)$$

Now one should take linear combinations of mobile and immobile differential equations such that only one equilibrium reaction rate of a kind happens in the whole set of equations. By subtracting block (3.29) from block (3.26), block (3.30) from block (3.27), and block (3.31) from block (3.27) only one of each equilibrium reaction rates will appear in the whole system. One \mathbf{r}_{mob} in (3.25), $\mathbf{r}_{sorp,li}$ in (3.29), $\mathbf{r}_{sorp,ld}$ in (3.30), and \mathbf{r}_{min} in (3.31).

Considering that $\mathbf{r}_{sorp,li}$ and $\mathbf{r}_{sorp,ld}$ are subvectors of \mathbf{r}_{sorp} , and substituting the differential equations containing equilibrium reaction rates with their corresponding AEs, we get

$$\frac{\partial}{\partial t}(\theta^w \boldsymbol{\eta}) + L\boldsymbol{\eta} = 0 \quad (3.33)$$

$$\frac{\partial}{\partial t}(\theta^w \bar{\boldsymbol{\eta}}) = 0 \quad (3.34)$$

$$\frac{\partial}{\partial t}(\theta^w \boldsymbol{\xi}_{sorp}) + L\boldsymbol{\xi}_{sorp} = \frac{\partial}{\partial t}(\theta^w \bar{\boldsymbol{\xi}}_{sorp,li}) + \theta^w (\mathbf{A}_{1,sorp} - \mathbf{A}_{2,sorp,li}) \mathbf{r}_{kin}(\mathbf{c}, \bar{\mathbf{c}}) \quad (3.35)$$

$$\begin{aligned} \frac{\partial}{\partial t}(\theta^w \boldsymbol{\xi}_{min}) + L\boldsymbol{\xi}_{min} &= \frac{\partial}{\partial t}(\theta^w \bar{\boldsymbol{\xi}}_{min}) + \mathbf{A}_{ld} \frac{\partial}{\partial t}(\theta^w \bar{\boldsymbol{\xi}}_{sorp,ld}) \\ &+ \theta^w (\mathbf{A}_{1,min} - \mathbf{A}_{ld} \mathbf{A}_{2,sorp,ld}) \mathbf{r}_{kin}(\mathbf{c}, \bar{\mathbf{c}}) \end{aligned} \quad (3.36)$$

$$\frac{\partial}{\partial t}(\theta^w \boldsymbol{\xi}_{kin}) + L\boldsymbol{\xi}_{kin} = \theta^w \mathbf{A}_{1,kin} \mathbf{r}_{kin}(\mathbf{c}, \bar{\mathbf{c}}) \quad (3.37)$$

$$\frac{\partial}{\partial t}(\theta^w \bar{\boldsymbol{\xi}}_{kin}) = \theta^w \mathbf{A}_{2,kin} \mathbf{r}_{kin} \quad (3.38)$$

$$\phi_{mob}(\mathbf{c}) = 0 \quad (3.39)$$

$$\phi_{sorp}(\mathbf{c}, \bar{\mathbf{c}}_{nmin}) = 0 \quad (3.40)$$

$$\phi_{min}(\mathbf{c}, \bar{\mathbf{c}}_{min}) = 0. \quad (3.41)$$

The blocks (3.33) and (3.34) are solved at the beginning of each time step independently from the rest of the equations. If porosity is constant, the block (3.34) remains constant during the course of the simulation. The blocks (3.38)-(3.41) are solved before the blocks (3.35)-(3.37). Since the blocks (3.38)-(3.41) do not contain any space derivative, they are called local equations and are solved locally (point-based) and their solutions are substituted in the block (3.35)-(3.37).

The blocks (3.35) and (3.36) contain more than one time derivative, hence the additional variables are introduced

$$\begin{aligned} \frac{\partial}{\partial t}(\theta^w \tilde{\boldsymbol{\xi}}_{sorp}) &= \frac{\partial}{\partial t}(\theta^w \boldsymbol{\xi}_{sorp}) - \frac{\partial}{\partial t}(\theta^w \bar{\boldsymbol{\xi}}_{sorp,li}) \\ \frac{\partial}{\partial t}(\theta^w \tilde{\boldsymbol{\xi}}_{min}) &= \frac{\partial}{\partial t}(\theta^w \boldsymbol{\xi}_{min}) - \frac{\partial}{\partial t}(\theta^w \bar{\boldsymbol{\xi}}_{min}) - \mathbf{A}_{ld} \frac{\partial}{\partial t}(\theta^w \bar{\boldsymbol{\xi}}_{sorp,ld}) \end{aligned} \quad (3.42)$$

where $\tilde{\boldsymbol{\xi}}_{sorp}$ and $\tilde{\boldsymbol{\xi}}_{min}$ are reaction invariants with respect to equilibrium reactions. The defining equations 3.42 are evaluated node-wise and added to the system of equations (3.33)-(3.41).

So the retransformation 3.17 can be written as

$$\begin{aligned} \mathbf{c} &= \mathbf{S}_{1,mob} \boldsymbol{\xi}_{mob} + \mathbf{S}_{1,sorp,li} \tilde{\boldsymbol{\xi}}_{sorp} + \mathbf{S}_{1,sorp} \bar{\boldsymbol{\xi}}_{sorp} \\ &+ \mathbf{S}_{1,min} (\tilde{\boldsymbol{\xi}}_{min} + \bar{\boldsymbol{\xi}}_{min}) + \mathbf{S}_{1,kin}^* \boldsymbol{\xi}_{kin} + \mathbf{S}_1^\perp \boldsymbol{\eta}, \\ \bar{\mathbf{c}} &= \begin{pmatrix} \mathbf{S}_{2,sorp} \bar{\boldsymbol{\xi}}_{sorp} + \mathbf{S}_{2,kin}^* \bar{\boldsymbol{\xi}}_{kin} \\ \bar{\boldsymbol{\xi}}_{min} \end{pmatrix} + \mathbf{S}_2^\perp \bar{\boldsymbol{\eta}}. \end{aligned} \quad (3.43)$$

The reaction extents are divided to global (primary variables) and local (secondary variables) unknowns as

$$\boldsymbol{\xi}_{glob} := \begin{pmatrix} \tilde{\boldsymbol{\xi}}_{sorp} \\ \tilde{\boldsymbol{\xi}}_{min} \\ \boldsymbol{\xi}_{sorp} \\ \boldsymbol{\xi}_{min} \\ \boldsymbol{\xi}_{kin} \end{pmatrix} \quad \boldsymbol{\xi}_{loc} := \begin{pmatrix} \boldsymbol{\xi}_{mob} \\ \bar{\boldsymbol{\xi}}_{sorp} \\ \bar{\boldsymbol{\xi}}_{min} \\ \bar{\boldsymbol{\xi}}_{kin} \end{pmatrix}. \quad (3.44)$$

Assuming the solution of η equations (3.33) and (3.34) are known and using local chemical solver for the solution of equations (3.38)-(3.41), the system of equations (3.33)-(3.41) can be reduced to

$$\tilde{\boldsymbol{\xi}}_{sorp} = \boldsymbol{\xi}_{sorp} - \bar{\boldsymbol{\xi}}_{sorp,li}(\tilde{\boldsymbol{\xi}}_{sorp}, \tilde{\boldsymbol{\xi}}_{min}, \boldsymbol{\xi}_{kin}) \quad (3.45)$$

$$\begin{aligned} \tilde{\boldsymbol{\xi}}_{min} &= \boldsymbol{\xi}_{min} - \bar{\boldsymbol{\xi}}_{min}(\tilde{\boldsymbol{\xi}}_{sorp}, \tilde{\boldsymbol{\xi}}_{min}, \boldsymbol{\xi}_{kin}) \\ &\quad - \mathbf{A}_{ld} \bar{\boldsymbol{\xi}}_{sorp,ld}(\tilde{\boldsymbol{\xi}}_{sorp}, \tilde{\boldsymbol{\xi}}_{min}, \boldsymbol{\xi}_{kin}) \end{aligned} \quad (3.46)$$

$$\frac{\partial}{\partial t}(\theta^w \tilde{\boldsymbol{\xi}}_{sorp}) + L \boldsymbol{\xi}_{sorp} = \theta^w (\mathbf{A}_{1,sorp} - \mathbf{A}_{2,sorp,li}) \mathbf{r}_{kin}(\tilde{\boldsymbol{\xi}}_{sorp}, \tilde{\boldsymbol{\xi}}_{min}, \boldsymbol{\xi}_{kin}) \quad (3.47)$$

$$\frac{\partial}{\partial t}(\theta^w \tilde{\boldsymbol{\xi}}_{min}) + L \boldsymbol{\xi}_{min} = \theta^w (\mathbf{A}_{1,min} - \mathbf{A}_{ld} \mathbf{A}_{2,sorp,ld}) \mathbf{r}_{kin}(\tilde{\boldsymbol{\xi}}_{sorp}, \tilde{\boldsymbol{\xi}}_{min}, \boldsymbol{\xi}_{kin}) \quad (3.48)$$

$$\frac{\partial}{\partial t}(\theta^w \boldsymbol{\xi}_{kin}) + L \boldsymbol{\xi}_{kin} = \theta^w \mathbf{A}_{1,kin} \mathbf{r}_{kin}(\tilde{\boldsymbol{\xi}}_{sorp}, \tilde{\boldsymbol{\xi}}_{min}, \boldsymbol{\xi}_{kin}) \quad (3.49)$$

which is used for numerical computations.

3.2.2.3 Local Chemical Solver

The defining nonlinear AEs and ODEs (3.38)-(3.41) of $\boldsymbol{\xi}_{loc}$

$$\begin{aligned} \phi_{mob}(\mathbf{c}) &= 0 \\ \phi_{sorp}(\mathbf{c}, \bar{\mathbf{c}}_{nmin}) &= 0 \\ \phi_{min}(\mathbf{c}, \bar{\mathbf{c}}_{min}) &= 0 \\ \frac{\theta^w \bar{\boldsymbol{\xi}}_{kin} - (\theta^w \bar{\boldsymbol{\xi}}_{kin})_{old}}{\Delta t} &= \theta^w \mathbf{A}_{2,kin} \mathbf{r}_{kin}(\mathbf{c}, \bar{\mathbf{c}}) \end{aligned}$$

are solved in the local chemical solver using a Newton iteration with line search. In order to improve the condition number of Jacobian matrix and avoid negative concentrations, natural log of concentrations of nonminerals are used. Mineral concentration should be able to reach zero because minimum function is used for evaluation of the complementarity condition. Therefore the concentration of mineral is not used in logarithm form. Since concentrations are used as unknowns ($I + \bar{I}$) in the local chemical solver, the defining equations of $\boldsymbol{\xi}_{glob}$ ($I + \bar{I} - J_{mob} - J_{sorp} - J_{min}$) are added to equal the number of equations with the number

of unknowns. Furthermore, the current time step values of ξ_{glob} , η and $\bar{\eta}$ act as constraints in evaluation of residual of the local chemical solver.

$$\phi_{mob}(\mathbf{l}) = 0 \quad (3.50)$$

$$-\eta + \left(\left(\mathbf{S}_1^{\perp T} \mathbf{S}_1^{\perp} \right)^{-1} \mathbf{S}_1^{\perp T} \exp(\mathbf{l}) \right) = 0 \quad (3.51)$$

$$\begin{aligned} -\tilde{\xi}_{sorp} + \left(\left(\mathbf{S}_1^{*T} \mathbf{S}_1^* \right)^{-1} \mathbf{S}_1^{*T} \exp(\mathbf{l}) \right)_{i=J_{mob}+1, \dots, J_{mob}+J_{sorp,li}} \\ - \left(\left(\mathbf{S}_2^{*T} \mathbf{S}_2^* \right)^{-1} \mathbf{S}_2^{*T} \left(\begin{array}{c} \exp(\bar{\mathbf{l}}_{nmin}) \\ \bar{\mathbf{c}}_{min} \end{array} \right) \right)_{i=1, \dots, J_{sorp,li}} = 0 \end{aligned} \quad (3.52)$$

$$\begin{aligned} -\tilde{\xi}_{min} + \left(\left(\mathbf{S}_1^{*T} \mathbf{S}_1^* \right)^{-1} \mathbf{S}_1^{*T} \exp(\mathbf{l}) \right)_{i=J_{mob}+J_{sorp,li}+1, \dots, J_{eq,li}} \\ - \bar{\mathbf{c}}_{min} - \mathbf{A}_{ld} \left(\left(\mathbf{S}_2^{*T} \mathbf{S}_2^* \right)^{-1} \mathbf{S}_2^{*T} \left(\begin{array}{c} \exp(\bar{\mathbf{l}}_{nmin}) \\ \bar{\mathbf{c}}_{min} \end{array} \right) \right)_{i=J_{sorp,li}+1, \dots, J_{sorp}} = 0 \end{aligned} \quad (3.53)$$

$$-\xi_{kin} + \left(\left(\mathbf{S}_1^{*T} \mathbf{S}_1^* \right)^{-1} \mathbf{S}_1^{*T} \exp(\mathbf{l}) \right)_{i=J_{eq,li}+1, \dots, J_{eq,li}+J_{1,kin}^*} = 0 \quad (3.54)$$

$$\phi_{sorp}(\mathbf{l}, \bar{\mathbf{l}}_{nmin}) = 0 \quad (3.55)$$

$$\phi_{min}(\mathbf{l}, \bar{\mathbf{c}}_{min}) = 0 \quad (3.56)$$

$$-\bar{\eta} + \left(\left(\mathbf{S}_2^{\perp T} \mathbf{S}_2^{\perp} \right)^{-1} \mathbf{S}_2^{\perp T} \left(\begin{array}{c} \exp(\bar{\mathbf{l}}_{nmin}) \\ \bar{\mathbf{c}}_{min} \end{array} \right) \right) = 0 \quad (3.57)$$

$$-\bar{\xi}_{kin} + \left(\left(\mathbf{S}_2^{*T} \mathbf{S}_2^* \right)^{-1} \mathbf{S}_2^{*T} \left(\begin{array}{c} \exp(\bar{\mathbf{l}}_{nmin}) \\ \bar{\mathbf{c}}_{min} \end{array} \right) \right)_{i=J_{sorp}+J_{min}+1, \dots, J_{sorp}+J_{min}+J_{2,kin}^*} = 0 \quad (3.58)$$

$$\frac{\theta^w \bar{\xi}_{kin} - (\theta^w \bar{\xi}_{kin})_{old}}{\Delta t} - \theta^w \mathbf{A}_{2,kin} \mathbf{r}_{kin}(\exp(\mathbf{l}), \exp(\bar{\mathbf{l}}_{nmin}), \bar{\mathbf{c}}_{min}) = 0 \quad (3.59)$$

with $J_{eq,li} = J_{mob} + J_{sorp,li} + J_{min}$. After solving the local problem the local variables ξ_{mob} and $\bar{\xi}_{sorp}$ are calculated using equation (3.17) as

$$\xi_{mob} = \left(\left(\mathbf{S}_1^{*T} \mathbf{S}_1^* \right)^{-1} \mathbf{S}_1^{*T} \mathbf{c} \right)_{i=1, \dots, J_{mob}}, \quad \bar{\xi}_{sorp} = \left(\left(\mathbf{S}_2^{*T} \mathbf{S}_2^* \right)^{-1} \mathbf{S}_2^{*T} \bar{\mathbf{c}} \right)_{i=1, \dots, J_{sorp}}$$

and $\bar{\xi}_{min}$ equals $\bar{\mathbf{c}}_{min}$. If a mineral is not present (total dissolution), the corresponding AE equation (3.59) is eliminated. The status of each mineral is stored in \mathbf{AI} vector. If solid mineral is present ($AI_j = 1$), the minimum is attained in the first argument of $\min\{\psi_j(\mathbf{c}), \bar{\mathbf{c}}_{min,j}\}$ and the reaction is called inactive and otherwise called active ($AI_j = 0$).

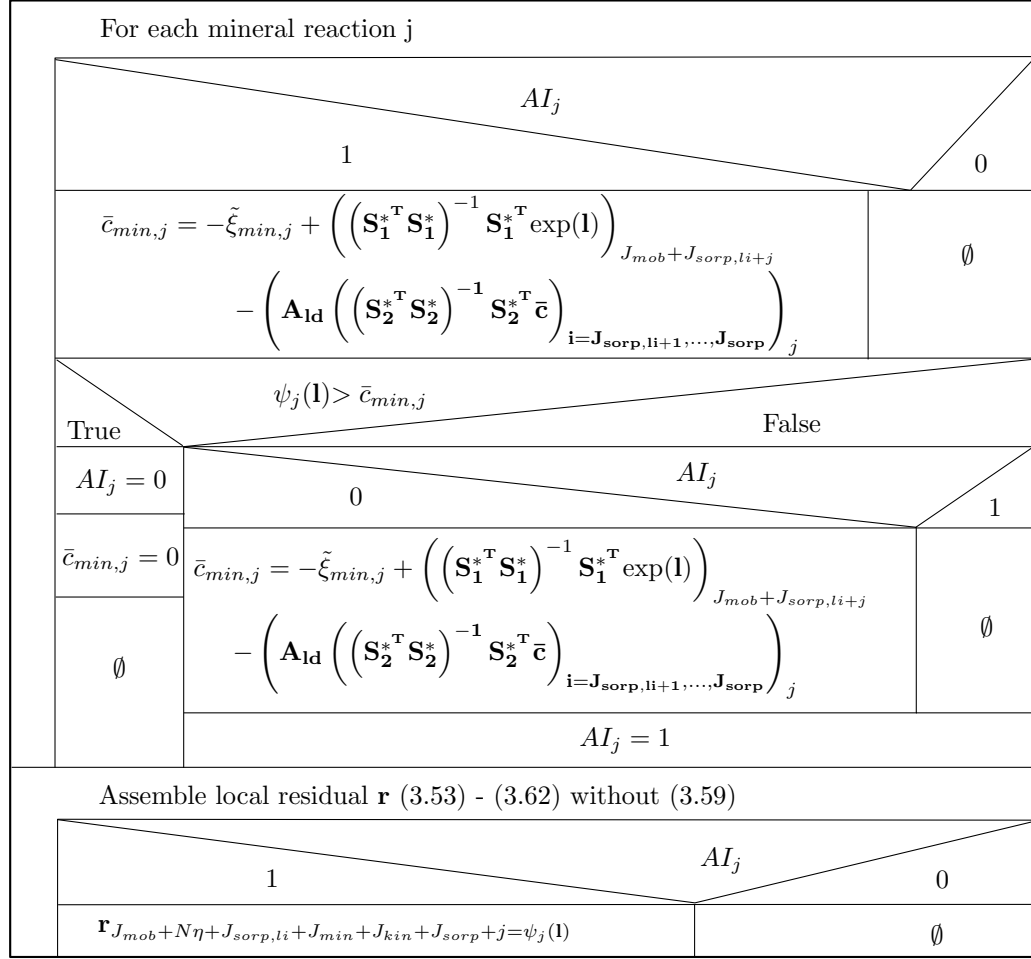


FIGURE 3.1: Algorithm applied for calculating the local residual.

3.3 Space and Time Discretization

The system of linear (3.33) and nonlinear partial differential equations (3.47)-(3.49) are solved numerically using finite element method (FEM) in space. Implicit Euler method is used for time discretization of (3.47)-(3.49). These numerical methods are briefly introduced in the following subsections.

3.3.1 Finite Element Method

A generic reactive mass transport equation reads

$$\frac{\partial}{\partial t}(\theta^w c) + \nabla \cdot (\mathbf{q}c - \theta^w \mathbf{D} \nabla c) = \theta^w r(c) \quad (3.60)$$

where the state variables are the concentrations c and reaction rates $r(c)$. In order to solve this equation numerically, the computational domain is discretized into finite number of elements in

$l =$ Maximum number of line search steps
Calculate residual vector \mathbf{r}
$d = \ \mathbf{r}\ $
Convergence criteria are not fulfilled
Assemble Jacobian Matrix \mathbf{J}
Solve linear system $\mathbf{J}\Delta\mathbf{x} = \mathbf{r}$
Update $\mathbf{x}^- = \Delta\mathbf{x}$
Calculate residual vector \mathbf{r}
$j = 0$
$j < l$
$d_1 = \ \mathbf{r}\ $
True $d_1 < d$ False
Break \emptyset
$\Delta\mathbf{x}^* = 0.5, \mathbf{x}^+ = \Delta\mathbf{x}$
Calculate residual vector \mathbf{r}
$j = j + 1$
$d = d_1$

FIGURE 3.2: Algorithm used for modified Newton's method with line search.

FEM ($\Omega = \bigcup_{e=1}^{ne} \Omega^e$) and interpolation (shape or basis) functions are used to compute the state variables within the elements ($\hat{c} = \sum_{j=1}^{nn} c_j N_j, \hat{r} = \sum_{j=1}^{nn} r_j N_j$).

Integrating the equation (3.60) over the entire domain and multiplying by a weighting function (Method of Weighted Residual) yields

$$\int_{\Omega} \left(\frac{\partial}{\partial t} (\theta^w \hat{c}) + \nabla \cdot (\mathbf{q}\hat{c} - \theta^w \mathbf{D}\nabla\hat{c}) \right) \omega_i d\Omega = \int_{\Omega} (\theta^w \hat{r}) \omega_i d\Omega \quad i = 1, \dots, nn. \quad (3.61)$$

Using Galerkin finite element, where the weighting function equals basis function ($N_j = \omega_i$), the equation (3.61) reads

$$\begin{aligned} \sum_{j=1}^{nn} \frac{\partial}{\partial t} c_j \int_{\Omega} N_i \theta^w N_j d\Omega + \sum_{j=1}^{nn} c_j \int_{\Omega} N_i \mathbf{q} \cdot \nabla N_j d\Omega - \sum_{j=1}^{nn} c_j \int_{\Omega} N_i \nabla \cdot (\theta^w \mathbf{D}\nabla N_j) d\Omega \\ = \sum_{j=1}^{nn} r_j \int_{\Omega} N_j \theta^w N_i d\Omega \quad i = 1, \dots, nn. \end{aligned} \quad (3.62)$$

Applying the Green's theorem (partial integration across the element boundaries) to the diffusive flux yields the semi-discrete weak form

$$\begin{aligned} \sum_{j=1}^{nn} \frac{\partial}{\partial t} c_j \int_{\Omega} N_i \theta^w N_j d\Omega + \sum_{j=1}^{nn} c_j \int_{\Omega} N_i \mathbf{q} \cdot \nabla N_j d\Omega + \sum_{j=1}^{nn} c_j \int_{\Omega} \theta^w \nabla N_i \cdot \mathbf{D}\nabla N_j d\Omega \\ = \sum_{j=1}^{nn} r_j \int_{\Omega} N_j \theta^w N_i d\Omega + \sum_{j=1}^{nn} c_j \int_{\Gamma} N_i \theta^w \mathbf{D}\nabla N_j \cdot \mathbf{n} d\Gamma \quad i = 1, \dots, nn, \end{aligned} \quad (3.63)$$

where \mathbf{n} is the outer normal vector. Dirichlet (Γ_D) and Neumann (Γ_N) boundary conditions are considered

$$\begin{aligned} c_i &= c_{D,i} && \text{on } \Gamma_D \\ \mathbf{D}\nabla c_i \cdot \mathbf{n} &= 0 && \text{on } \Gamma_N \end{aligned}$$

such that $\Gamma = \Gamma_D \dot{\cup} \Gamma_N$. Boundary conditions are required for η , ξ_{sorp} , ξ_{min} and ξ_{kin} variables.

3.3.2 Time Discretization

Implicit Euler method is used for time integration. The linear interpolation between old (t^{old}) and new (t) time steps is applied to concentrations, mass fluxes and source/sink terms. Hence, the time derivative is approximated as

$$\frac{\partial}{\partial t} c \approx \frac{\Delta c}{\Delta t} = \frac{c - c^{old}}{t - t^{old}}. \quad (3.64)$$

The fully discrete form reads

$$\begin{aligned} & \sum_{j=1}^{nn} \frac{c_j - c_j^{old}}{t - t^{old}} \int_{\Omega} N_i \theta^w N_j d\Omega + \sum_{j=1}^{nn} c_j \int_{\Omega} N_i \mathbf{q} \cdot \nabla N_j d\Omega + \sum_{j=1}^{nn} c_j \int_{\Omega} \theta^w \nabla N_i \cdot \mathbf{D}\nabla N_j d\Omega \\ &= \sum_{j=1}^{nn} r_j \int_{\Omega} N_j \theta^w N_i d\Omega + \sum_{j=1}^{nn} c_j \int_{\Gamma} N_i \theta^w \mathbf{D}\nabla N_j \cdot \mathbf{n} d\Gamma \quad i = 1, \dots, nn, \end{aligned} \quad (3.65)$$

Mass lumping

In order to improve the stability of the method, mass lumping is applied to diagonalize the mass matrix (mass is concentrated on the discretization nodes)

$$M_{i,i} = \sum_{k=1}^{nn} m_{i,k}.$$

The corresponding entries of mass matrix, conductance matrix and source/sink terms are divided by each diagonal entry of mass matrix ($M_{i,i}$) to convert the mass matrix to identity matrix which is equivalent to division by porosity.

3.3.3 Jacobian Matrix

It is assumed that $\mathbf{f}(\boldsymbol{\xi}_{glob}, \boldsymbol{\xi}_{loc})$ correspond to global problem and equations $\mathbf{g}(\boldsymbol{\xi}_{glob}, \boldsymbol{\xi}_{loc})$ correspond to local problem after space and time discretizations. Since $\boldsymbol{\xi}_{loc}$ is a function of $\boldsymbol{\xi}_{glob}$ (due to application of local chemical solver), the system of discretized equations can be written as

$$\mathbf{f}(\boldsymbol{\xi}_{glob}, \boldsymbol{\xi}_{loc}(\boldsymbol{\xi}_{glob})) = 0 \quad (3.66)$$

$$\mathbf{g}(\boldsymbol{\xi}_{glob}, \boldsymbol{\xi}_{loc}(\boldsymbol{\xi}_{glob})) = 0. \quad (3.67)$$

The evaluation of Jacobian matrix and $\boldsymbol{\xi}_{loc}(\boldsymbol{\xi}_{glob})$ are required for the solution of equations (3.66) with Newton iteration. The evaluation of the local problems $\mathbf{g}(\boldsymbol{\xi}_{glob}, \boldsymbol{\xi}_{loc})$ for fixed $\boldsymbol{\xi}_{glob}$ is performed in local chemical solver as explained in subsection 3.2.2.3. The Jacobian matrix is

$$J = \frac{\partial \mathbf{f}}{\partial \boldsymbol{\xi}_{glob}} + \frac{\partial \mathbf{f}}{\partial \boldsymbol{\xi}_{loc}} \frac{\partial \boldsymbol{\xi}_{loc}}{\partial \boldsymbol{\xi}_{glob}} \quad (3.68)$$

where $\frac{\partial \boldsymbol{\xi}_{loc}}{\partial \boldsymbol{\xi}_{glob}}$ is evaluated by taking the derivative of (3.67) with respect to $\boldsymbol{\xi}_{glob}$ as

$$\frac{\partial \mathbf{g}}{\partial \boldsymbol{\xi}_{loc}} \frac{\partial \boldsymbol{\xi}_{loc}}{\partial \boldsymbol{\xi}_{glob}} = - \frac{\partial \mathbf{g}}{\partial \boldsymbol{\xi}_{glob}}. \quad (3.69)$$

In order to solve $\frac{\partial \boldsymbol{\xi}_{loc}}{\partial \boldsymbol{\xi}_{glob}}$, mineral reactions are split into inactive (index I) and active (index A) reactions as explained in 3.2.2.3

$$\mathbf{S}_{1,min} = (\mathbf{S}_{1,min,I}, \mathbf{S}_{1,min,A}).$$

The change of $\bar{\boldsymbol{\xi}}_{kin}$ is much smaller compared to $\boldsymbol{\xi}_{mob}$, $\bar{\boldsymbol{\xi}}_{sorp}$, and $\bar{\boldsymbol{\xi}}_{min}$, accordingly, the approximation $D_{\boldsymbol{\xi}_{glob}} \bar{\boldsymbol{\xi}}_{kin} \approx 0$ is made. Furthermore, since $\boldsymbol{\xi}_{sorp}$ and $\boldsymbol{\xi}_{min}$ do not appear in the retransformation (3.43), they are neglected in $\boldsymbol{\xi}_{glob}$ vector. The derivative of local equation with respect to local variables are needed

$$\frac{\partial \mathbf{g}}{\partial \boldsymbol{\xi}_{loc}} = \begin{pmatrix} \mathbf{B}^T \tilde{\boldsymbol{\Lambda}} \mathbf{B} & * \\ \mathbf{0} & \mathbf{I}_A \end{pmatrix}$$

where $\mathbf{B}^T \tilde{\boldsymbol{\Lambda}} \mathbf{B}$ includes $\frac{\partial \phi_{min,I}}{\partial \boldsymbol{\xi}_{min,I}}$, with

$$\mathbf{B} = \begin{pmatrix} \mathbf{S}_{1,mob} & \mathbf{S}_{1,sorp} & \mathbf{S}_{1,min,I} \\ \mathbf{0} & \mathbf{S}_{2,sorp} & \mathbf{0} \end{pmatrix}, \quad \tilde{\boldsymbol{\Lambda}} = \begin{pmatrix} \boldsymbol{\Lambda} & \mathbf{0} \\ \mathbf{0} & \bar{\boldsymbol{\Lambda}}_{nmin} \end{pmatrix}$$

and the diagonal matrices

$$\Lambda = \begin{pmatrix} 1/c_1 & & \mathbf{0} \\ & \ddots & \\ \mathbf{0} & & 1/c_I \end{pmatrix}, \quad \bar{\Lambda}_{nmin} = \begin{pmatrix} 1/\bar{c}_{I+1} & & \mathbf{0} \\ & \ddots & \\ \mathbf{0} & & 1/\bar{c}_{I+\bar{I}_{nmin}} \end{pmatrix}.$$

Analogously $-\frac{\partial \mathbf{g}}{\partial \xi_{glob}}$ is calculated

$$-\frac{\partial \mathbf{g}}{\partial \xi_{glob}} = \begin{pmatrix} \mathbf{B}^T \tilde{\Lambda} \mathbf{C} \\ \mathbf{0} \end{pmatrix}$$

with

$$\mathbf{C} = \begin{pmatrix} -\mathbf{S}_{1,sorp,li} & -\mathbf{S}_{1,min} & -\mathbf{S}_{1,kin}^* \\ \mathbf{0} & \mathbf{0} & \mathbf{0} \end{pmatrix}$$

Due to the structure of $\frac{\partial \mathbf{g}}{\partial \xi_{loc}}$ and $\frac{\partial \mathbf{g}}{\partial \xi_{glob}}$, the matrix containing the derivative of local variables w.r.t global variables has a structure as $\frac{\partial \xi_{loc}}{\partial \xi_{glob}} = \begin{pmatrix} \mathbf{X} \\ \mathbf{0} \end{pmatrix}$, where the upper block \mathbf{X} consists of $D_{\xi_{glob}} \bar{\xi}_{min,I}$ the lower block consists of $D_{\xi_{glob}} \bar{\xi}_{min,A}$. The Matrix \mathbf{X} is the solution of the linear systems

$$\mathbf{B}^T \tilde{\Lambda} \mathbf{B} \mathbf{X} = \mathbf{B}^T \tilde{\Lambda} \mathbf{C}. \quad (3.70)$$

The global Jacobian matrix (3.68) is constructed as

$$\frac{\partial \mathbf{f}}{\partial \xi_{glob}} = \begin{pmatrix} \mathbf{I} & \mathbf{0} & -\mathbf{I} & \mathbf{0} & \mathbf{0} \\ \mathbf{0} & \mathbf{I} & \mathbf{0} & -\mathbf{I} & \mathbf{0} \\ \theta^w \mathbf{I} & \mathbf{0} & \Delta t \mathbf{L}_h & \mathbf{0} & \mathbf{0} \\ \mathbf{0} & \theta^w \mathbf{I} & \mathbf{0} & \Delta t \mathbf{L}_h & \mathbf{0} \\ \mathbf{0} & \mathbf{0} & \mathbf{0} & \mathbf{0} & \theta^w \mathbf{I} + \Delta t \mathbf{L}_h \end{pmatrix} - \Delta t \theta^w \begin{pmatrix} \mathbf{0} & \mathbf{0} & \mathbf{0} & \mathbf{0} & \mathbf{0} \\ \mathbf{0} & \mathbf{0} & \mathbf{0} & \mathbf{0} & \mathbf{0} \\ \mathbf{A}_{sorp} D_{\xi_{sorp}} \tilde{\mathbf{r}}_{kin} & \mathbf{A}_{sorp} D_{\xi_{min}} \tilde{\mathbf{r}}_{kin} & \mathbf{0} & \mathbf{0} & \mathbf{A}_{sorp} D_{\xi_{kin}} \tilde{\mathbf{r}}_{kin} \\ \mathbf{A}_{min} D_{\xi_{sorp}} \tilde{\mathbf{r}}_{kin} & \mathbf{A}_{min} D_{\xi_{min}} \tilde{\mathbf{r}}_{kin} & \mathbf{0} & \mathbf{0} & \mathbf{A}_{min} D_{\xi_{kin}} \tilde{\mathbf{r}}_{kin} \\ \mathbf{A}_{1,kin} D_{\xi_{sorp}} \tilde{\mathbf{r}}_{kin} & \mathbf{A}_{1,kin} D_{\xi_{min}} \tilde{\mathbf{r}}_{kin} & \mathbf{0} & \mathbf{0} & \mathbf{A}_{1,kin} D_{\xi_{kin}} \tilde{\mathbf{r}}_{kin} \end{pmatrix}$$

with $\mathbf{A}_{sorp} := \mathbf{A}_{1,sorp} - \mathbf{A}_{2,sorp,li}$, $\mathbf{A}_{min} := \mathbf{A}_{1,min} - \mathbf{A}_{ld}\mathbf{A}_{2,sorp,ld}$ and \mathbf{L}_h the discretization of the transport operator L .

$$\frac{\partial \mathbf{f}}{\partial \xi_{loc}} = \begin{pmatrix} \mathbf{0} & \mathbf{I} & \mathbf{0} & \mathbf{0} \\ \mathbf{0} & \mathbf{0} & \mathbf{A}_{ld} & \mathbf{0} \\ -\Delta t \theta^w \mathbf{A}_{sorp} D_{(\xi_{mob}, \bar{\xi}_{sorp,li}, \bar{\xi}_{sorp,ld}, \bar{\xi}_{min})} \mathbf{r}^{kin} & & & \\ -\Delta t \theta^w \mathbf{A}_{min} D_{(\xi_{mob}, \bar{\xi}_{sorp,li}, \bar{\xi}_{sorp,ld}, \bar{\xi}_{min})} \mathbf{r}^{kin} & & & \\ -\Delta t \theta^w \mathbf{A}_{1,kin} D_{(\xi_{mob}, \bar{\xi}_{sorp,li}, \bar{\xi}_{sorp,ld}, \bar{\xi}_{min})} \mathbf{r}^{kin} & & & \end{pmatrix}$$

multiplication with $\frac{\partial \xi_{loc}}{\partial \xi_{glob}}$ gives

$$\frac{\partial \mathbf{f}}{\partial \xi_{loc}} \frac{\partial \xi_{loc}}{\partial \xi_{glob}} = \begin{pmatrix} D_{\bar{\xi}_{sorp}} \bar{\xi}_{sorp,li} & D_{\bar{\xi}_{min}} \bar{\xi}_{sorp,li} & \mathbf{0} & \mathbf{0} & D_{\xi_{kin}} \bar{\xi}_{sorp,li} \\ D_{\bar{\xi}_{sorp}} \bar{\xi}_{min} + \mathbf{A}_{ld} D_{\bar{\xi}_{sorp}} \bar{\xi}_{sorp,ld} & D_{\bar{\xi}_{min}} \bar{\xi}_{min} + \mathbf{A}_{ld} D_{\bar{\xi}_{min}} \bar{\xi}_{sorp,ld} & \mathbf{0} & \mathbf{0} & D_{\xi_{kin}} \bar{\xi}_{min} + \mathbf{A}_{ld} D_{\xi_{kin}} \bar{\xi}_{sorp,ld} \\ \mathbf{R}_{sorp} D_{\bar{\xi}_{sorp}} (\xi_{mob}, \bar{\xi}_{sorp}, \bar{\xi}_{min}) & \mathbf{R}_{sorp} D_{\bar{\xi}_{min}} (\xi_{mob}, \bar{\xi}_{sorp}, \bar{\xi}_{min}) & \mathbf{0} & \mathbf{0} & \mathbf{R}_{sorp} D_{\xi_{kin}} (\xi_{mob}, \bar{\xi}_{sorp}, \bar{\xi}_{min}) \\ \mathbf{R}_{min} D_{\bar{\xi}_{sorp}} (\xi_{mob}, \bar{\xi}_{sorp}, \bar{\xi}_{min}) & \mathbf{R}_{min} D_{\bar{\xi}_{min}} (\xi_{mob}, \bar{\xi}_{sorp}, \bar{\xi}_{min}) & \mathbf{0} & \mathbf{0} & \mathbf{R}_{min} D_{\xi_{kin}} (\xi_{mob}, \bar{\xi}_{sorp}, \bar{\xi}_{min}) \\ \mathbf{R}_{kin} D_{\bar{\xi}_{sorp}} (\xi_{mob}, \bar{\xi}_{sorp}, \bar{\xi}_{min}) & \mathbf{R}_{kin} D_{\bar{\xi}_{min}} (\xi_{mob}, \bar{\xi}_{sorp}, \bar{\xi}_{min}) & \mathbf{0} & \mathbf{0} & \mathbf{R}_{kin} D_{\xi_{kin}} (\xi_{mob}, \bar{\xi}_{sorp}, \bar{\xi}_{min}) \end{pmatrix}$$

with

$$\mathbf{R}_{sorp} := -\Delta t \theta^w \mathbf{A}_{sorp} D_{(\xi_{mob}, \bar{\xi}_{sorp,li}, \bar{\xi}_{sorp,ld}, \bar{\xi}_{min})} \mathbf{r}^{kin}$$

$$\mathbf{R}_{min} := -\Delta t \theta^w \mathbf{A}_{min} D_{(\xi_{mob}, \bar{\xi}_{sorp,li}, \bar{\xi}_{sorp,ld}, \bar{\xi}_{min})} \mathbf{r}^{kin}$$

$$\mathbf{R}_{kin} := -\Delta t \theta^w \mathbf{A}_{1,kin} D_{(\xi_{mob}, \bar{\xi}_{sorp,li}, \bar{\xi}_{sorp,ld}, \bar{\xi}_{min})} \mathbf{r}^{kin}.$$

Solve η problem
Solve local problem ξ_{loc}
Calculate residual \mathbf{r} of the global problem
Convergence criteria of global problem not fulfilled
Assemble Jacobian Matrix \mathbf{J} of the global problem
Solve linear system $\mathbf{J} \Delta \xi_{glob} = \mathbf{r}$
Update $\xi_{glob} = \Delta \xi_{glob}$
Solve local problem ξ_{loc}
Calculate residual \mathbf{r} of the global problem

FIGURE 3.3: One time step of the reduction scheme.

TABLE 3.1: Solvers and preconditioners used to solve the system of linear equations in each benchmark.

Benchmark	Solver	Preconditioner
Cation exchange	direct solver	-
Calcite dissolution-precipitation	GMRES	ILU
Mixing controlled biodegradation	BICGSTAB	ILU

3.4 Code Implementation

The GIA or one step method with the reduction technique is implemented into the new version of OpenGeoSys (OGS⁶) software. Semi-smooth Newton method is used to solve the nonlinear equation systems. For the local nonlinear AEs and ODEs, Newton iteration with line search is applied. Conformal Finite Elements are used for space discretization. Mass lumping is applied in mass matrix. Reaction rate terms, mass and conductance matrices are normalized by mass matrix.

Implicit Euler method is used for time discretization. An adaptive time stepping scheme is applied where the time step size is determined by the number of Newton steps in the previous time step. If Newton method fails to converge, the current time step will be repeated with a smaller step size. If convergence is achieved within a few Newton iterations (typically < 3), the Δt will be increased in the next time step.

The global linear system can be solved by either iterative (*e.g.* SpBiCGSTAB, SpQMRCGSTAB) or direct (*e.g.* SpGAUSS) solvers with preconditioner (*e.g.* Jacobi, ILU and SOR) in OGS⁶. Table 3.1 shows a list of solvers and preconditioners used to solve the system of linear equations in each benchmark.

The differential equations associated with equilibrium reactions are replaced by algebraic equations based on law of mass action (LMA) and kinetic rate terms are expressed by double Monod expression. Debye-Hückel and its extension Davies equations are implemented to calculate the activity coefficients used in LMA. Equivalent algebraic equation of CCs is solved replacing the equations containing equilibrium mineral reaction rates. Jacobian of local Newton method with line search is evaluated numerically and natural logarithms of non-mineral concentrations are used in local chemical solvers.

Chapter 4

Benchmarks

4.1 Introduction

A series of benchmark tests for verification of the implemented code is presented in this chapter. In order to measure the efficiency of the GIA with reduction scheme, results are compared with the results obtained with SNIA.

4.2 Cation Exchange

The cation exchange benchmark was proposed as example 11 in the PHREEQC manual [PA⁺99], and also previously applied to verify the coupling of OGS⁵-PHREEQC [KGSW12]. In this benchmark, a 1D column of length 0.08m is considered. Initially the column contains a Na-K-NO₃⁻ solution in equilibrium with the cation exchanger X. CaCl₂ is continuously injected into the column for a period of one day (3 pore volumes). Ca²⁺, K⁺, and Na⁺ react in equilibrium with the exchanger during the simulation, whereas Cl⁻ is only transported along the column as a tracer. Table 4.1 shows the flow and transport parameters used in this benchmark. The chemical reaction system is presented in Table 4.2 where NaX, KX and CaX are secondary sorbed species. A total exchange capacity of 1.1 mmol/l is considered for the exchanger X. Capon convention [Spo08] is used to calculate activity of the sorbed species in OGS⁶. Debye-Hückel equation is employed to calculate the activity coefficients of aqueous species. A space discretization of 1mm and time discretization of 120s are used for both simulations to reduce numerical dispersion and improve the convergence of the Newton's approach. The convergence tolerance is set to 1×10^{-9} for the Newton iteration and 1×10^{-14} for linear solver.

Figure 4.1 shows the breakthrough curves of the simulated concentrations at the end of the column. They were simulated by OGS⁶ and OGS⁵-PHREEQC after 3 pore volumes. Both

TABLE 4.1: Model setup parameters used in cation exchange benchmark.

Parameter	Value	Unit
Column length	0.08	m
Effective porosity	0.5	-
Bulk density	2000	kg/m ³
Longitudinal dispersion length	0.002	m
Darcy velocity	2.78×10^{-6}	m/s

TABLE 4.2: Chemical reaction system used in cation exchange benchmark

Chemical reactions	Log ₁₀ K values
$K^+ + NaX = KX + Na^+$	0.7
$\frac{1}{2}Ca^{2+} + NaX = CaX + Na^+$	0.4

codes produced nearly identical results. Cl^- as conservative tracer breaks through after about one pore volume. Na^+ is initially present in the domain and is replaced by incoming Ca^{2+} . K^+ is replaced by Ca^{2+} after the desorption of Na^+ . After all K^+ is released, the concentration of Ca^{2+} reaches steady-state value.

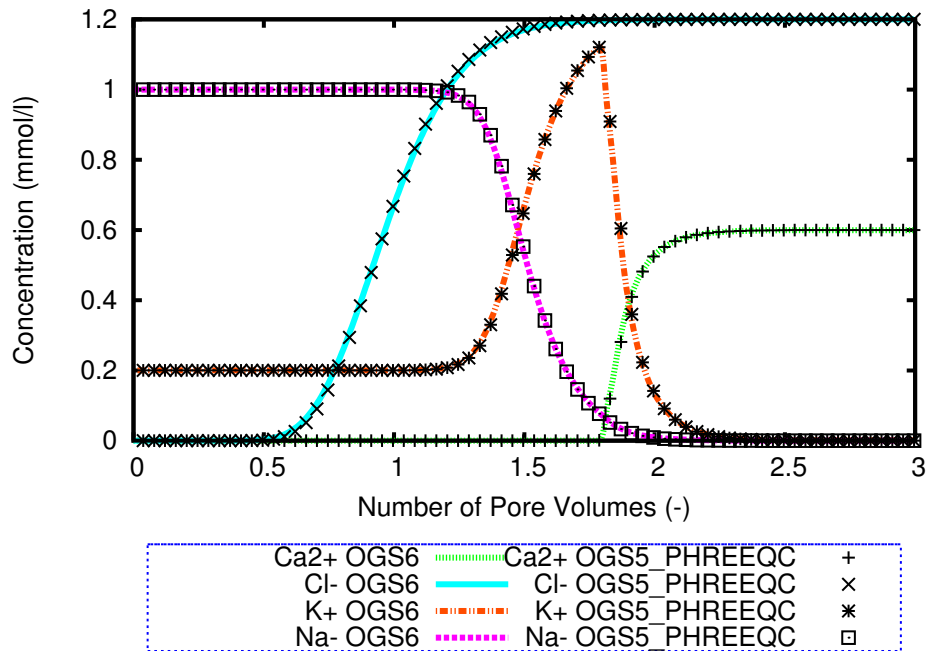


FIGURE 4.1: Simulated breakthrough curves of concentrations in the cation exchange benchmark. Results produced by OGS⁶ using GIA and OGS⁵-PHREEQC for 3 pore volumes.

TABLE 4.3: Model parameters used in mineral dissolution and precipitation benchmark.

Parameter	Value	Unit
Column length	0.5	m
Effective porosity	0.32	-
Bulk density	1800	kg/m ³
Longitudinal dispersion length	0.0067	m
Pore velocity	9.375×10^{-6}	m/s

TABLE 4.4: Chemical reaction system for mineral dissolution and precipitation benchmark

Chemical reactions	Log ₁₀ K values
$\text{H}^+ + \text{CO}_3^{2-} = \text{HCO}_3^-$	10.3289
$\text{Ca}^{2+} + \text{CO}_3^{2-} = \text{CaCO}_3$	3.2241
$\text{Ca}^{2+} + \text{H}^+ + \text{CO}_3^{2-} = \text{CaHCO}_3^+$	11.4346
$\text{Mg}^{2+} + \text{CO}_3^{2-} = \text{MgCO}_3$	2.9797
$\text{Mg}^{2+} + \text{H}^+ + \text{CO}_3^{2-} = \text{MgHCO}_3^+$	11.3971
$\text{CO}_3^{2-} + \text{Ca}^{2+} = \text{CaCO}_3(\text{s})$	8.4799
$2\text{CO}_3^{2-} + \text{Ca}^{2+} + \text{Mg}^{2+} = \text{CaMg}(\text{CO}_3)_2(\text{s})$	16.5398

4.3 Dissolution and Precipitation

A hypothetical scenario of 1D mass transport and calcite dissolution and dolomite precipitation is considered. Engesgaard and Kipp [EK92] proposed this benchmark for the model verification of MST1D, and Prommer [Pro02] later used it for the model verification of PHT3D code. A one dimensional column with initially 2.17×10^{-5} mol/kg calcite mineral is considered. The column is flushed with MgCl_2 solution at an aqueous concentration of 1.0×10^{-3} mol/l, leading to development of multiple precipitation/dissolution fronts. As the solution front proceeds into the column, calcite mineral dissolves and dolomite mineral precipitates temporally. Reaction feedback on permeability and porosity is ignored due to the low amount of precipitation/dissolution of minerals. Table 4.3 and 4.4 show the model setup parameters and chemical reactions considered, respectively. A mesh size of 5mm is considered for all simulations. Time discretization of 100s ($\text{Cr} = 0.06$ [-]) is chosen for SNIA to control the numerical dispersion during simulations. The simulation time in all variant configurations are set to 21000 seconds. The convergence tolerance is set to 1×10^{-7} for Newton iteration and 1×10^{-14} for linear solver.

Figures 4.2 and 4.3 shows the aqueous concentration and mineral abundance profiles, respectively. Cl^- is considered to be a tracer and not taking part in the reactions. As the same groundwater velocity is applied, three different codes yield same Cl^- . During the first 48 minutes of simulation, SNIA of OGS⁶ could not capture the behavior of dolomite mineral properly (results are not shown). This could be due to the small concentration of dolomite at early stage of simulation and splitting error in SNIA. All results are comparable after the first hour of simulation.

GIA simulated slightly sharper fronts and tails for aqueous and mineral concentration profiles compared to SNIA (SNIA module of OGS⁶ and OGS⁵-PHREEQC). The major difference is most observable on the dissolution tail of dolomite between OGS⁶ and OGS⁵-PHREEQC codes. In order to assess the efficiency of GIA with reduction scheme in simulating homogeneous equilibrium reactions, calcite and dolomite minerals are removed from the chemical system, and the simulations are run with the same parameters.

The CPU time for the GIA and SNIA of OGS⁶ are compared in figure 4.4. The x axis shows the number of mesh nodes in kilo and y axis the CPU time in kilo seconds.

SNIA of OGS⁶ is approximately 4.7 times faster than GIA with reduction scheme in simulating mineral dissolution-precipitation (heterogeneous equilibrium reactions). GIA with reduction scheme, however, is approximately 6.7 times faster than SNIA in simulating aqueous equilibrium reactions (homogeneous equilibrium reactions). Homogeneous equilibrium reactions are treated as local problems and are solved node wise in the local chemical solver. Hence, in homogeneous equilibrium chemical reaction systems, no global Newton iteration is performed which is the reason of 6.7 times efficiency of GIA with reduction scheme compared to SNIA.

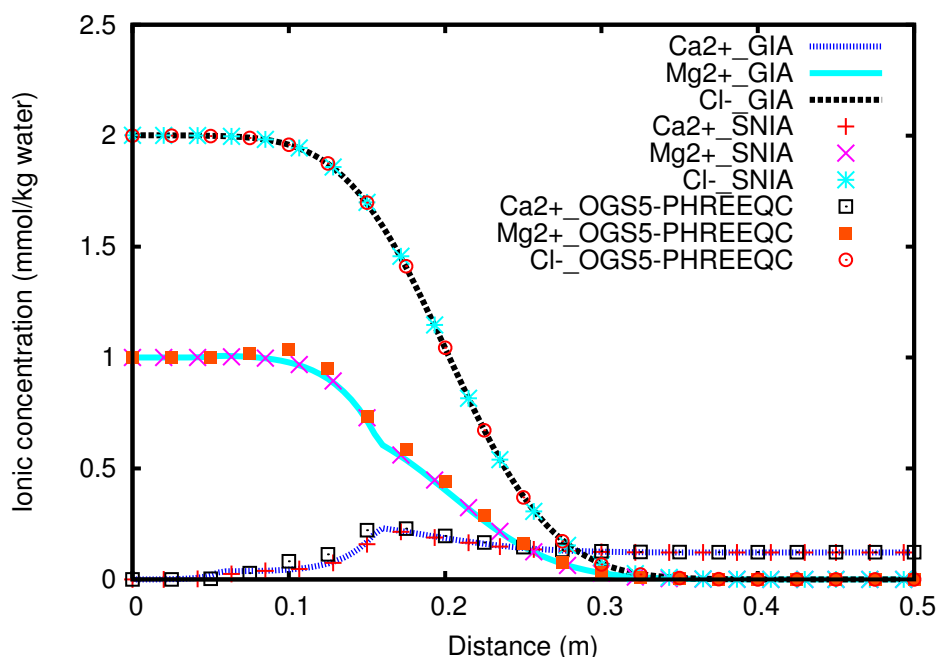


FIGURE 4.2: Simulated aqueous concentration profiles after 21000s for GIA and SNIA of OGS⁶ and OGS⁵-PHREEQC.

4.4 Mixing Controlled Biodegradation

Biodegradation of contaminants is limited by the availability of the electron donor and acceptor substrates. Assuming a steady-state flow field, the mixing of the reactants is controlled by

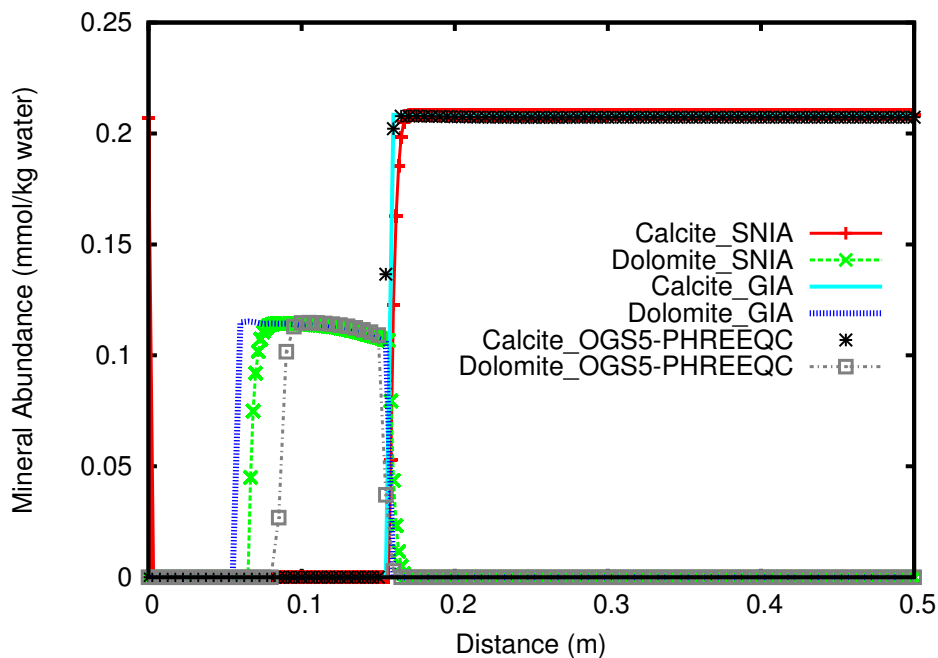


FIGURE 4.3: Calcite and dolomite profiles produced by GIA and SNIA of OGS⁶ and OGS⁵-PHREEQC after 21000s.

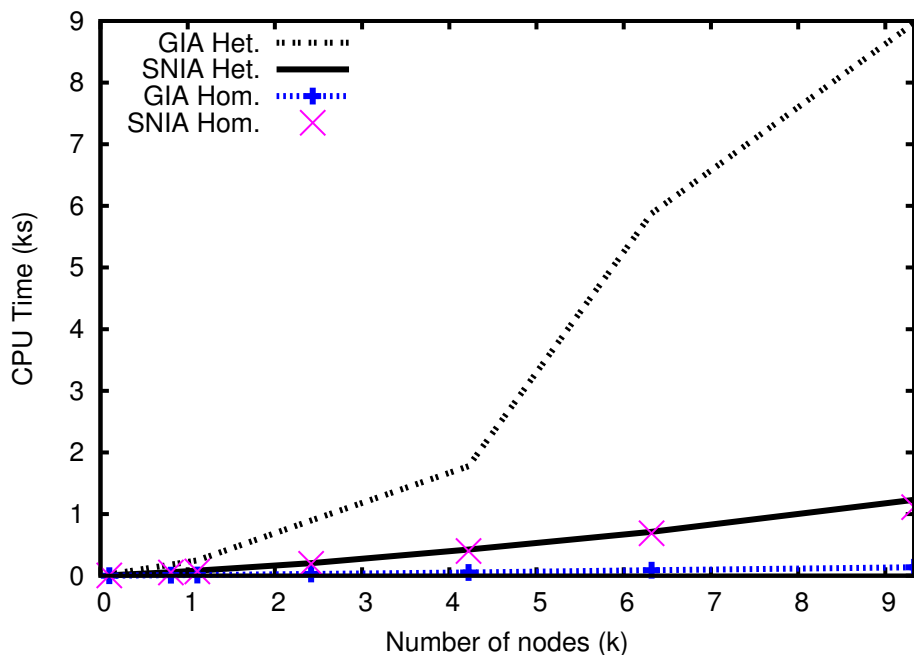


FIGURE 4.4: CPU time measured versus number of nodes in simulating mineral dissolution and precipitation benchmark for GIA and SNIA of OGS⁶. All simulations are run on Intel(R) Core(TM) i5-2520M CPU running at 2.50GHz.

transverse dispersion. Cirpka and Valocchi [CV07] presented an analytical solution to calculate the steady-state dissolved compounds and biomass distribution due to transverse dispersion in porous media. Their analytical solution was later revised and improved [SCDB⁺09, CV09].

The new analytical solution was then used by Centler et al. [CSDB⁺10] for model verification of GeoSysBRNS code.

Figure 4.5 shows the model domain with 5m length and 0.2m width. A steady-state groundwater flow is considered where the water flows along the x axis with the velocity of 1 m/d. The porosity is 0.5 and transverse and longitudinal dispersion coefficient of 2.5 and 250 cm²/d are considered, respectively. Biodegradation reaction of the form $A + B \rightarrow C$ is considered. Electron acceptor B (e.g. oxygen) is continuously injected to the domain at a concentration of 2.5×10^{-4} mol/l along the left boundary ($x=0$) except a 0.05m section in the center of the inflow boundary, where the carbon source A is entering the domain at a concentration of 3.3×10^{-4} mol/l. The kinetic reaction depends on the availability of the electron donor (compound A) and electron acceptor (compound B) in the presence of the biomass. The kinetic rate is expressed by double-Monod kinetics with biomass ($R = \frac{c_A}{K_A+c_A} \frac{c_B}{K_B+c_B} \frac{\mu_{max}}{Y} C_{bio}$). Biomass decays with constant first order rate parameter K_{dec} ($\frac{\partial}{\partial t} C_{bio} = \frac{c_A}{K_A+c_A} \frac{c_B}{K_B+c_B} \mu_{max} C_{bio} - K_{dec} C_{bio}$). Table 4.5 shows the parameters used to simulate this benchmark.

Different modules of OGS⁶, namely GIA with local chemical solver using first order backward Euler method for ODEs, GIA with ODE solver, and SNIA, is used to simulate this benchmark. Bulirsch-Stör algorithm is used to solve the ODE systems. Model run time of 100 days is chosen to approach steady state condition. The domain is discretized in 2.5 cm in x-direction and 5 mm in y-direction. In the SNIA case, temporal discretization of 120 s is chosen to control the splitting error. In the GIA case, adaptive time stepping scheme is applied. A minimum step size of 120 s and maximum time step size of 8640 s is used for GIA with reduction scheme. The convergence tolerance is set to 1×10^{-9} for global Newton, 1×10^{-12} for local Newton, and 1×10^{-14} for linear solvers.

Figure 4.6 shows the transverse distribution of substrates A, B, and product C and Figure 4.7 shows the transverse distribution of biomass at 1 m distance down gradient of the inflow boundary. All three modules of OGS⁶ produced comparable results. Simulation run times, however, are different for different modules. Figure 4.8 shows the time required for GIA and SNIA to simulate mixing controlled biodegradation benchmark. GIA with reduction scheme using backward Euler method, ODE solvers are on average 23 and 58.1 times faster than SNIA.

TABLE 4.5: Model parameters for the mixing controlled biodegradation benchmark.

Symbol	Parameter	Value	Unit
K_A	Monod constant substrate A	8.33×10^{-5}	m/L
K_B	Monod constant substrate B	3.13×10^{-5}	m/L
μ_{max}	Maximum growth rate	1.0	1/d
K_{dec}	Biomass death rate	0.1	1/d
Y	Yield coefficient	1.0	g/mol
v_a	Transport velocity	1.0	m/d
α_l	Longitudinal dispersion length	2.5	cm
α_t	Transverse dispersion length	2.5×10^{-2}	cm

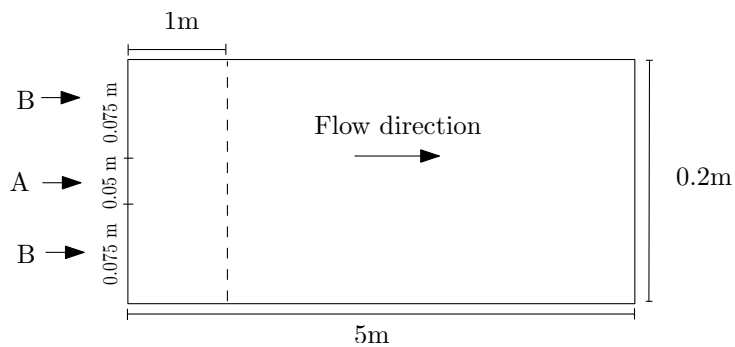
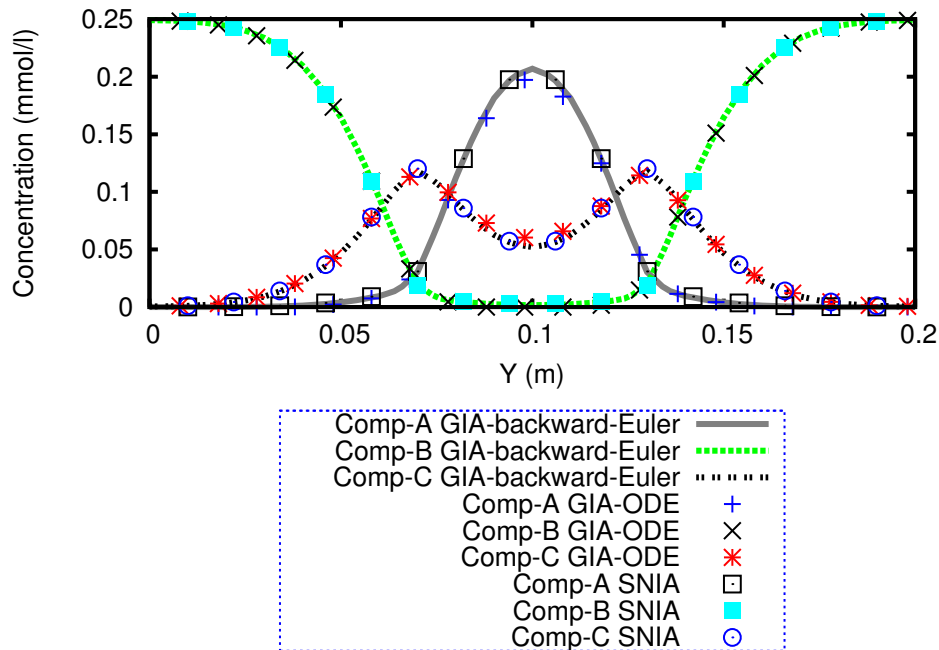
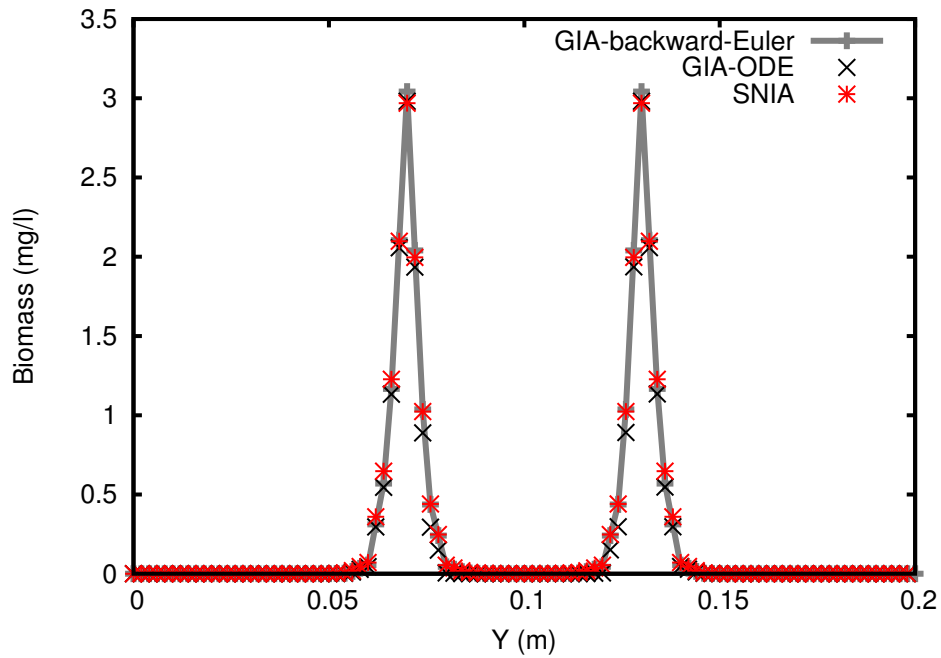
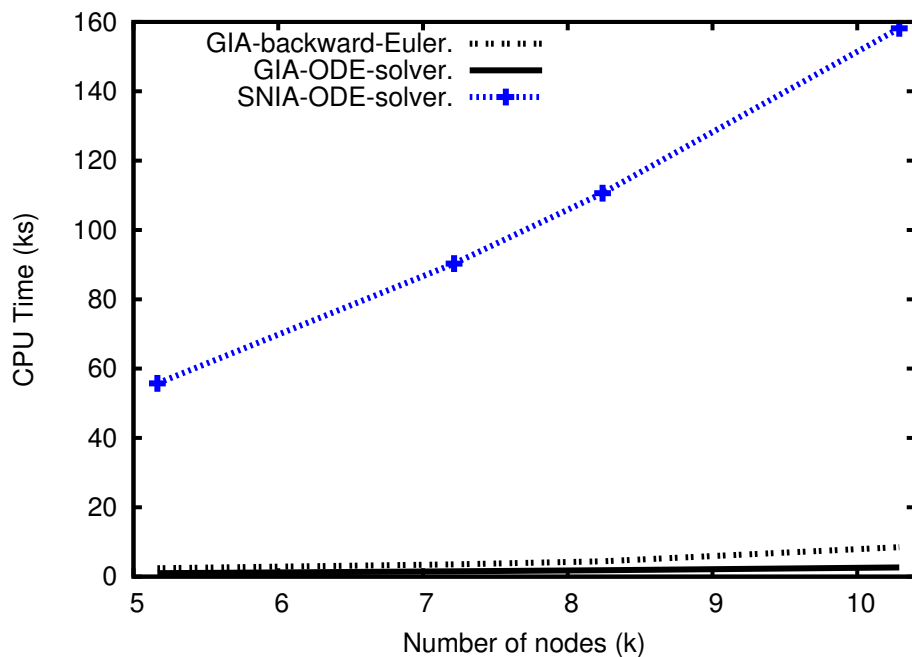


FIGURE 4.5: Simulation domain for mixing controlled biodegradation benchmark. Break-through curves are plotted along the cross section at 1m distance from the inlet.

FIGURE 4.6: Transverse profiles of compounds A, B and C at $x = 1$ m for GIA and SNIA of OGS⁶.

FIGURE 4.7: Transverse profiles of biomass at $x = 1\text{m}$ for GIA and SNIA of OGS⁶.FIGURE 4.8: CPU time measured versus number of mesh nodes in simulating mixing controlled biodegradation benchmark with GIA and SNIA of OGS⁶. All simulations are run on a computer with Intel(R) Xeon(R) CPU X5650 clocking at 2.67GHz.

Chapter 5

Conclusions and Outlooks

5.1 Conclusions

GIA with reduction scheme proposed by Krättele [KK05, Hof10] was implemented into the OpenGeoSys (OGS⁶) software and some test cases were run for accuracy and efficiency comparison between GIA with the reduction scheme and SNIA.

Cation exchange benchmark as a heterogeneous equilibrium reaction was simulated by GIA with reduction scheme of OGS⁶ and OGS⁵-PHREEQC codes. The result of both codes were identical, implying the correct implementation of GIA with reduction scheme in OGS⁶ software for simulating such equilibrium heterogeneous reactions.

Mineral precipitation/dissolution benchmark was run for different domains with increasing number of mesh nodes. Since there is no analytical solutions for such a complex chemical system, the results of OGS⁶ were compared to the ones obtained with OGS⁵-PHREEQC code. The simulation results of all three codes are comparable. There are some differences in the dissolution tails of dolomite mineral profiles obtained with three different methods which might be due to the different implementation methods and numerical and splitting errors. It was observed that even for small number of nodes SNIA outperforms GIA with reduction scheme in solving heterogeneous equilibrium mineral reactions in the absence of kinetic reactions. SNIA was on average ca. 4.7 faster than GIA in simulating mineral precipitation/dissolution benchmark. GIA with reduction scheme produced the sharpest fronts in aqueous and solid phases whereas concentration fronts are smoother in SNIA.

It should be noted that the efficiency results are measured for either equilibrium or kinetic reaction systems. These results might differ in a mixed equilibrium and kinetic reaction system depending on simulation run time.

GIA with reduction scheme is on average ca. 6.7 times faster than SNIA in simulating homogeneous equilibrium reactions. This efficiency is due to the lack of global nonlinear PDEs which requires the largest computation resources and simpler chemistry system in the local chemical solver.

Time step size restriction due to avoidance of numerical and OS errors has negative impact on computational time efficiency of SNIA in long simulation runs of kinetic reaction systems. This point was shown in mixing controlled biodegradation benchmark with simulation run time of 100 days. GIA with reduction scheme using chemical solvers took almost 1.2 hours whereas SNIA required up to 29.7 hours with similar results.

The findings can be summarized in the following points:

- For simulating heterogeneous reactions SNIA, despite time step size limitation, tends to be on average 4.7 times faster than GIA (section 4.3, Figure 4.4). The inefficiency of GIA with reduction scheme is due to computation burden of Jacobian matrix and transport operator in each Newton iteration.
- GIA with reduction scheme is on average 6.7 times faster than SNIA in simulating homogeneous equilibrium reactions (section 4.3, Figure 4.4). The efficiency of GIA in such systems comes from the lack of Newton iteration for global nonlinear PDEs and simpler chemistry system in the local chemical solvers.
- GIA with reduction scheme is 24 times faster than SNIA in long term simulation of kinetic reactions in mixing controlled biodegradation benchmark (section 4.4, Figure 4.8). GIA is more efficient than SNIA due to taking larger time step sizes in simulations with long run times.

5.2 Outlooks

For future works the following points can be considered

- Field scale mixed equilibrium and kinetic reaction scenario for a better comparison between GIA with the reduction scheme and SNIA.
- Implement kinetic mineral reactions in the complimentary condition instead of law of mass action.
- Extend the code to consider gas phase.
- Consider the effects of density and temperature on flow system and chemical reactions.

Bibliography

- [AM63] Rutherford Aris and RHS Mah. Independence of chemical reactions. *Industrial & Engineering Chemistry Fundamentals*, 2(2):90–94, 1963.
- [Bea72] J. Bear. Dynamics of fluids in porous media, 764 pp. *American Elsevier, New York*, 1972.
- [Bet07] Craig M Bethke. *Geochemical and biogeochemical reaction modeling*. Cambridge University Press, 2007.
- [BKKK11] H. Buchholzer, C. Kanzow, P. Knabner, and S. Krättele. The semismooth newton method for the solution of reactive transport problems including mineral precipitation-dissolution reactions. *Computational Optimization and Applications*, 50(2):193–221, 2011.
- [CHK⁺10] J. Carrayrou, J. Hoffmann, P. Knabner, S. Krättele, C. De Dieuleveult, J. Erhel, J. Van der Lee, V. Lagneau, K. U. Mayer, and K. T.B. MacQuarrie. Comparison of numerical methods for simulating strongly nonlinear and heterogeneous reactive transport problems the momas benchmark case. *Computational Geosciences*, 14(3):483–502, 2010.
- [CMB04] J. Carrayrou, R. Mosé, and P. Behra. Operator-splitting procedures for reactive transport and comparison of mass balance errors. *Journal of Contaminant Hydrology*, 68(3):239–268, 2004.
- [CSDB⁺10] F. Centler, H. Shao, C. De Biase, C.H. Park, P. Regnier, O. Kolditz, and M. Thullner. Geosysbrnsa flexible multidimensional reactive transport model for simulating biogeochemical subsurface processes. *Computers & Geosciences*, 36(3):397–405, 2010.
- [CV07] O. A. Cirpka and A. J. Valocchi. Two-dimensional concentration distribution for mixing-controlled bioreactive transport in steady state. *Advances in water resources*, 30(6):1668–1679, 2007.

- [CV09] O. A. Cirpka and A. J. Valocchi. Reply to comments on two-dimensional concentration distribution for mixing-controlled bioreactive transport in steady state by h. shao et al. *Advances in Water Resources*, 32(2):298–301, 2009.
- [EK92] P. Engesgaard and K. L. Kipp. A geochemical transport model for redox-controlled movement of mineral fronts in groundwater flow systems: A case of nitrate removal by oxidation of pyrite. *Water Resources Research*, 28(10):2829–2843, 1992.
- [FR92] J. C. Friedly and J. Rubin. Solute transport with multiple equilibrium-controlled or kinetically controlled chemical reactions. *Water Resources Research*, 28(7):1935–1953, 1992.
- [Fri91] J. C. Friedly. Extent of reaction in open systems with multiple heterogeneous reactions. *AIChE journal*, 37(5):687–693, 1991.
- [FYB03] Yilin Fang, Gour-Tsyh Yeh, and William D Burgos. A general paradigm to model reaction-based biogeochemical processes in batch systems. *Water Resources Research*, 39(4), 2003.
- [HK89] J. Herzer and W. Kinzelbach. Coupling of transport and chemical processes in numerical transport models. *Geoderma*, 44(2):115–127, 1989.
- [HKK10] Joachim Hoffmann, Serge Kräutle, and Peter Knabner. A parallel global-implicit 2-d solver for reactive transport problems in porous media based on a reduction scheme and its application to the momas benchmark problem. *Computational Geosciences*, 14(3):421–433, 2010.
- [HKK12] Joachim Hoffmann, Serge Kräutle, and Peter Knabner. A general reduction scheme for reactive transport in porous media. *Computational Geosciences*, 16(4):1081–1099, 2012.
- [Hof10] J. Hoffmann. *Reactive transport and mineral dissolution, precipitation in porous media: efficient solution algorithms, benchmark computations and existence of global solutions*. PhD thesis, Erlangen, Nurnberg, Univ., Diss., 2010, 2010.
- [KGSW12] O Kolditz, UJ Görke, H Shao, and W Wang. Thermo-hydro-mechanical-chemical processes in fractured porous media. *Lecture notes in computational science and engineering*, 86, 2012.
- [KK05] Serge Kräutle and Peter Knabner. A new numerical reduction scheme for fully coupled multicomponent transport-reaction problems in porous media. *Water resources research*, 41(9), 2005.

- [KK07] Serge Kräutle and Peter Knabner. A reduction scheme for coupled multicomponent transport-reaction problems in porous media: Generalization to problems with heterogeneous equilibrium reactions. *Water resources research*, 43(3), 2007.
- [KM95] Jagath J Kaluarachchi and Jahangir Morshed. Critical assessment of the operator-splitting technique in solving the advection-dispersion-reaction equation: 1. first-order reaction. *Advances in Water Resources*, 18(2):89–100, 1995.
- [Kol02] Olaf Kolditz. *Computational methods in environmental fluid mechanics*. Springer, 2002.
- [Krä08] Serge Kräutle. General multi-species reactive transport problems in porous media: efficient numerical approaches and existence of global solutions. *University of Erlangen-Nuremberg, Department of Mathematics, Erlangen*, 2008.
- [Krä11] Serge Kräutle. The semismooth newton method for multicomponent reactive transport with minerals. *Advances in Water Resources*, 34(1):137–151, 2011.
- [Las98] Antonio C Lasaga. *Kinetic theory in the earth sciences*. Princeton University Press, 1998.
- [MCAS04] Sergi Molins, Jesús Carrera, Carlos Ayora, and Maarten W Saaltink. A formulation for decoupling components in reactive transport problems. *Water Resources Research*, 40(10), 2004.
- [MK95] Jahangir Morshed and Jagath J Kaluarachchi. Critical assessment of the operator-splitting technique in solving the advection-dispersion-reaction equation: 2. monod kinetics and coupled transport. *Advances in Water Resources*, 18(2):101–110, 1995.
- [PA⁺99] David L Parkhurst, CAJ Appelo, et al. User’s guide to phreeqc (version 2): A computer program for speciation, batch-reaction, one-dimensional transport, and inverse geochemical calculations. 1999.
- [Pro02] H. Prommer. A reactive multicomponent transport model for saturated porous media, user’s manual version 1.0. 2002.
- [RK88] Howard Reeves and David J Kirkner. Multicomponent mass transport with homogeneous and heterogeneous chemical reactions: effect of the chemistry on the choice of numerical algorithm: 2. numerical results. *Water Resources Research*, 24(10):1730–1739, 1988.
- [Rub83] Jacob Rubin. Transport of reacting solutes in porous media: Relation between mathematical nature of problem formulation and chemical nature of reactions. *Water Resources Research*, 19(5):1231–1252, 1983.

- [SAC98] Maarten W Saaltink, Carlos Ayora, and Jesús Carrera. A mathematical formulation for reactive transport that eliminates mineral concentrations. *Water Resources Research*, 34(7):1649–1656, 1998.
- [SCA00] MW Saaltink, J Carrera, and C Ayora. A comparison of two approaches for reactive transport modelling. *Journal of Geochemical Exploration*, 69:97–101, 2000.
- [SCA01] Maarten W Saaltink, Jesus Carrera, and Carlos Ayora. On the behavior of approaches to simulate reactive transport. *Journal of Contaminant Hydrology*, 48(3):213–235, 2001.
- [SCDB+09] Haibing Shao, Florian Centler, Cecilia De Biase, Martin Thullner, and Olaf Kolditz. Comments on two-dimensional concentration distribution for mixing-controlled bioreactive transport in steady-state by oa cirpka and aj valocchi. *Advances in Water Resources*, 32(2):293–297, 2009.
- [SL94] Carl I Steefel and Antonio C Lasaga. A coupled model for transport of multiple chemical species and kinetic precipitation/dissolution reactions with application to reactive flow in single phase hydrothermal systems. *American Journal of Science*, 294(5):529–592, 1994.
- [SL06] Matthew J Simpson and Kerry A Landman. Characterizing and minimizing the operator split error for fishers equation. *Applied mathematics letters*, 19(7):604–612, 2006.
- [SL07] Matthew J Simpson and Kerry A Landman. Analysis of split operator methods applied to reactive transport with monod kinetics. *Advances in water resources*, 30(9):2026–2033, 2007.
- [SL08] Matthew J Simpson and Kerry A Landman. Theoretical analysis and physical interpretation of temporal truncation errors in operator split algorithms. *Mathematics and Computers in Simulation*, 77(1):9–21, 2008.
- [SM96] Carl I Steefel and Kerry TB MacQuarrie. Approaches to modeling of reactive transport in porous media. *Reviews in Mineralogy and Geochemistry*, 34(1):85–129, 1996.
- [SM12] Werner Stumm and James J Morgan. *Aquatic chemistry: chemical equilibria and rates in natural waters*, volume 126. John Wiley & Sons, 2012.
- [Spo08] Garrison Sposito. *The chemistry of soils*. Oxford university press, 2008.
- [VM92] Albert J Valocchi and Michael Malmstead. Accuracy of operator splitting for advection-dispersion-reaction problems. *Water Resources Research*, 28(5):1471–1476, 1992.

- [XSA⁺99] Tianfu Xu, Javier Samper, Carlos Ayora, Marisol Manzano, and Emilio Custodio. Modeling of non-isothermal multi-component reactive transport in field scale porous media flow systems. *Journal of Hydrology*, 214(1):144–164, 1999.
- [Yeh00] George Yeh. *Computational subsurface hydrology: Reactions, transport, and fate*, volume 2. Springer, 2000.
- [YT89] GT Yeh and VS Tripathi. A critical evaluation of recent developments in hydrogeochemical transport models of reactive multichemical components. *Water resources research*, 25(1):93–108, 1989.